Cell Reports
Medicine

Article

Fab and Fc contribute to maximal protection against SARS-CoV-2 following NVX-CoV2373 subunit vaccine with Matrix-M vaccination

Graphical abstract

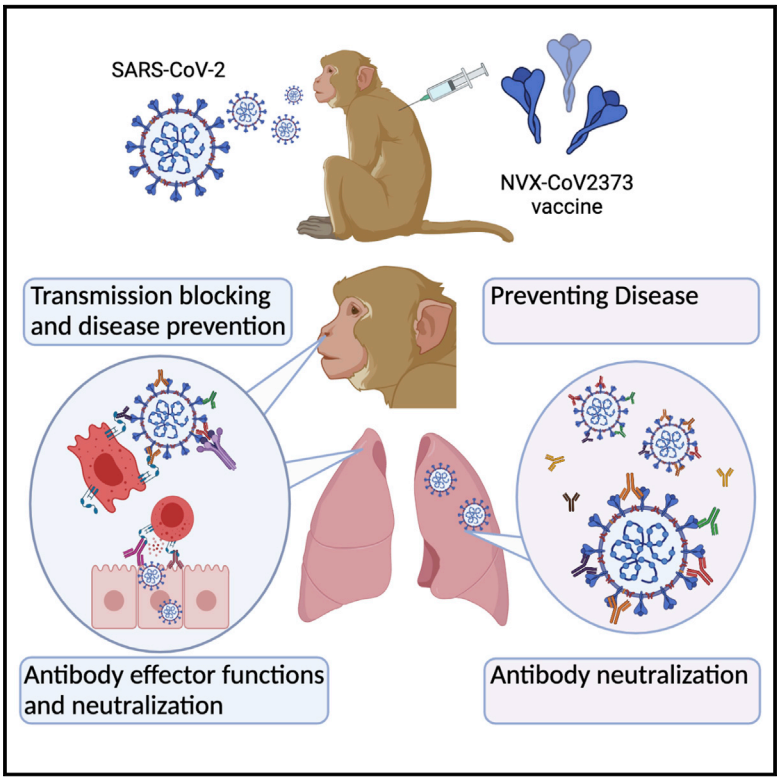

Authors

Matthew J. Gorman, Nita Patel, Mimi Guebre-Xabier, ..., Gregory Glenn, Gale Smith, Galit Alter

Correspondence

gsmith@novavax.com (G.S.), galter@mgh.harvard.edu (G.A.)

In brief

Gorman et al. demonstrate that both neutralization and Fc-effector functions are important in controlling SARS-CoV-2 infection in the respiratory tract after NVX-CoV2373 vaccination in non-human primates. In addition, the authors profile the humoral response in humans after NVX-CoV2373 vaccination and demonstrate altered Fc-receptor binding to emerging SARS-CoV-2 variants.

Highlights

- NVX-CoV2373 vaccine elicits neutralizing and Fc-effector functional antibodies
- The vaccine protects against respiratory tract infection in non-human primates
- Both neutralizing and Fc-effector functions contribute to protection
- Human vaccine-induced antibodies exhibit altered Fc-receptor binding to CoV-2 variants

Gorman et al., 2021, Cell Reports Medicine 2, 100405
September 21, 2021
https://doi.org/10.1016/j.xcrm.2021.100405

CellPress

Cell Reports Medicine

CellPress
OPEN ACCESS

Article

Fab and Fc contribute to maximal protection against SARS-CoV-2 following NVX-CoV2373 subunit vaccine with Matrix-M vaccination

Matthew J. Gorman,[1,11] Nita Patel,[2,11] Mimi Guebre-Xabier,[2,11] Alex L. Zhu,[1,3,11] Caroline Atyeo,[1,11] Krista M. Pullen,[4,11] Carolin Loos,[1,4,11] Yenny Goez-Gazi,[5] Ricardo Carrion, Jr.,[5] Jing-Hui Tian,[2] Dansu Yuan,[1] Kathryn A. Bowman,[1] Bin Zhou,[2] Sonia Maciejewski,[2] Marisa E. McGrath,[6] James Logue,[6] Matthew B. Frieman,[6] David Montefiori,[7] Colin Mann,[8] Sharon Schendel,[8] Fatima Amanat,[9] Florian Krammer,[9,10] Erica Ollmann Saphire,[8] Douglas A. Lauffenburger,[4] Ann M. Greene,[2] Alyse D. Portnoff,[2] Michael J. Massare,[2] Larry Ellingsworth,[2] Gregory Glenn,[2] Gale Smith,[2,*] and Galit Alter[1,12,*]

[1]Ragon Institute of MGH, MIT, and Harvard, Cambridge, MA 02139, USA
[2]Novavax, Inc., 21 Firstfield Road, Gaithersburg, MD 20878, USA
[3]Virology and Immunology Program, University of Duisburg-Essen, Essen, Germany
[4]Department of Biological Engineering, Massachusetts Institute of Technology, Cambridge, MA 02139, USA
[5]Texas Biomedical Research Institute, 8715 West Military Drive, San Antonio, TX 78227, USA
[6]University of Maryland School of Medicine, 685 West Baltimore St, Baltimore, MD 21201, USA
[7]Department of Surgery, Duke University Medical Center, Durham, NC 27710, USA
[8]La Jolla Institute for Immunology, La Jolla, CA 92037, USA
[9]Department of Microbiology, Icahn School of Medicine at Mount Sinai, New York, NY, USA
[10]Department of Pathology, Icahn School of Medicine at Mount Sinai, New York, NY, USA
[11]These authors contributed equally
[12]Lead contact
*Correspondence: gsmith@novavax.com (G.S.), galter@mgh.harvard.edu (G.A.)
https://doi.org/10.1016/j.xcrm.2021.100405

SUMMARY

Recently approved vaccines have shown remarkable efficacy in limiting SARS-CoV-2-associated disease. However, with the variety of vaccines, immunization strategies, and waning antibody titers, defining the correlates of immunity across a spectrum of antibody titers is urgently required. Thus, we profiled the humoral immune response in a cohort of non-human primates immunized with a recombinant SARS-CoV-2 spike glycoprotein (NVX-CoV2373) at two doses, administered as a single- or two-dose regimen. Both antigen dose and boosting significantly altered neutralization titers and Fc-effector profiles, driving unique vaccine-induced antibody fingerprints. Combined differences in antibody effector functions and neutralization were associated with distinct levels of protection in the upper and lower respiratory tract. Moreover, NVX-CoV2373 elicited antibodies that functionally targeted emerging SARS-CoV-2 variants. Collectively, the data presented here suggest that a single dose may prevent disease via combined Fc/Fab functions but that two doses may be essential to block further transmission of SARS-CoV-2 and emerging variants.

INTRODUCTION

SARS-CoV-2 causes a spectrum of disease, from asymptomatic to mild and severe coronavirus disease 2019 (COVID-19). Since it crossed into humans, the virus has spread globally with more than 150 million confirmed cases and more than 3 million deaths.[1] COVID-19 manifests with a range of clinical symptoms from asymptomatic to severe disease, with 50%–75% of infected individuals exhibiting asymptomatic infection, and only a small proportion (2%–5%) developing severe disease, requiring mechanical ventilation.[2–4] The vaccines authorized for emergency use in North America or Europe—mRNA-1273, Ad26.COV2.S, ChAdOx1 nCoV-19, and BNT162b2—have been successful in preventing severe infections and in inducing anti-SARS-CoV-2 $CD4^+$ T cells, $CD8^+$ T cells, and potent neutralizing-antibody responses.[5–9] Emerging data from Israel suggest the BNT162b2 vaccine is capable of reducing transmission;[10] however, whether all vaccines can confer protection against transmission and the durability and correlates of protection remain unclear.

Emerging phase 3 data suggest that vaccine-mediated protection emerges as early as 10 days after primary vaccination,[11,12] at a time when neutralizing antibodies are low or undetectable.[5–7] Because a significant fraction of the globe has delayed mRNA boosting to increase population-level immunity or have elected to deploy a single vaccine dose of Ad26, understanding the correlates of immunity after a single dose is critical. Moreover, with the imminent waning of vaccine-induced

immunity across platforms, understanding correlates of immunity across antibody titers may provide critical insights for boosting. Emerging correlates of immunity after administration of DNA- and adenoviral-vector SARS-CoV-2 vaccination point to a potential additional role for added antibody effector functions, in addition to neutralization, as key correlates of immunity against SARS-CoV-2.[13,14] However, whether functional responses evolve after both a prime and a boost, provide differential protection across the upper and lower respiratory tract, and provide protection against variants remain unclear.

In this study, we deeply interrogated humoral correlates of protection in a cohort of rhesus macaques immunized with one or two doses of 5 or 25 μg of a stabilized, recombinant, full-length SARS-CoV-2 spike (S) glycoprotein (NVX-CoV2373) with a 50-μg Matrix-M adjuvant (Novamax, Gaithersburg, MD, USA). Animals immunized with the two-dose regimen, regardless of whether given the high (25 μg) or low (5 μg) antigen dose, were protected against upper (URTI) and lower respiratory infection (LRTI) and shedding of replicating virus, whereas a single vaccine injection (regardless of antigen dose) was only partially protective against infection. Distinct combinations of Fc features and neutralizing antibody responses were associated with protection in the upper and lower respiratory tract, pointing to potential mechanistic differences required to control the virus at those distinct immunological locations. Critically, the NVX-CoV2373 generated binding and functional humoral immune responses to several emerging SARS-CoV-2 variants. These data point to a collaboration between the Fab and Fc that provides maximal protection against infection and transmission of SARS-CoV-2 and emerging mutants.

RESULTS

Subgenomic virus mRNA in respiratory samples

Prior studies using a two-dose immunization regimen of NVX-CoV2373 in cynomolgus macaques demonstrated significant neutralizing titers and protection in upper and lower airways after SARS-CoV-2 challenge.[15] However, emerging phase 3 data from mRNA vaccine platforms suggest that vaccine-induced protection against disease is observable as early as 10 days after vaccine priming, before the presence of peak neutralizing antibody levels.[11,12] In addition, whether protection is achievable with a single dose remains unclear. To define the specific humoral profiles that track with protective immunity against disease and infection, we profiled the humoral immune response induced by NVX-CoV2373 after a prime-only or prime/boost vaccine regimen administered at two different antigen doses (5 and 25 μg) with a Matrix-M adjuvant (50 μg). Groups of rhesus macaques (n = 5) were immunized with one vaccine dose (study day 0) or two vaccine doses spaced 3 weeks apart (study days 0 and 21). Control animals (n = 4) received one or two injections of formulation buffer (placebo). Serum was collected before immunization (day 0) and 21 and 31/32 days after the first dose (Figure 1A).

Protection was assessed by analyzing viral loads across the upper (nasal washes and nasopharyngeal swabs) and lower (bronchoalveolar lavage [BAL]) respiratory tract on days 2–8 post-infection (dpi). The highest levels of viral subgenomic RNA (sgRNA) were observed in placebo animals across the upper and lower-respiratory tract samples, with peak viral loads observed 2 dpi and persistent sgRNA until day 7/8 (Figures 1B–1D). Animals immunized with a single dose of 5 μg or 25 μg NVX-CoV2373 had lower levels of replicating virus at day 2 in all tissues except nasal pharyngeal swabs compared with placebo; however, the 25-μg dose was able to clear sgRNA in BAL and nasopharyngeal swabs by day 7/8, whereas the 5 μg only cleared BAL. The animals that received 5 μg or 25 μg antigen in a prime/boost regimen had no detectable viral loads in BAL or nasopharyngeal swabs at any day, and all sgRNA was cleared in nasal washes by day 4. In addition, tissue samples were collected from the upper, middle, and lower right lung lobes; trachea; and nasal cavity at the scheduled necropsy (7–8 dpi) and were analyzed for viral gRNA. There was no gRNA in the nasal cavity, trachea, or lungs of animals immunized with the 5-μg or 25-μg antigen in a prime/boost regimen (Figures 1E–1G). Conversely, nearly all placebo animals exhibited gRNA in each tissue (Figures 1E–1G). Animals immunized with a single vaccine dose were partially protected, with a few animals having detectable gRNA. These data suggest that one vaccine dose was able to induce a partially protective immune response, differing by antigen dose level, but two vaccine doses resulted in full protection against infection along the respiratory tract, independent of antigen dose.

Antibody responses after NVX-CoV2373 immunization

To determine whether the humoral immune response could distinguish protected from non-protected animals, we analyzed the immunoglobulin G (IgG) titers and neutralizing-antibody response across the vaccine groups. Robust anti-S IgG titers were observed across both vaccine groups after a single immunization. Anti-S IgG titers remained stable at 31/32 days after 1 dose; however, anti-S IgG titers significantly increased 21–35-fold within 10 days after the booster immunization with 5 μg or 25 μg of NVX-CoV2373 (Figure 2A). Low levels of mucosal anti-S IgG antibodies were detected in the nasal washes and BAL aspirates collected 31/32 days after one immunization, increasing 8–22-fold in nasal washes and BAL aspirates at 10 days after the booster immunization (Figures 2B and 2C).

To further profile the functional potential of the vaccine-induced antibodies, an S-pseudotype virus neutralization assay was used to assess the neutralizing capacity in the serum of immunized animals. Serum from animals immunized with 5 μg or 25 μg NVX-CoV2373 had similar pseudovirus-neutralizing titers (50% infective dose [ID_{50}]) after a single dose. After booster immunization, pseudovirus-neutralizing titers significantly increased, with no significant differences noted between the antigen doses (Figure 2D). In addition, live wild-type (WT) virus neutralization assays and human angiotensin-converting enzyme 2 (hACE2) inhibition exhibited similar trends, with detectable neutralization/inhibition at day 21 in all regimens, with a significant increase after the second vaccine dose (Figures 2E and 2F). Overall, these results indicate that NVX-CoV2373 administered as a prime/boost regimen elicited high anti-S IgG titers, capable of blocking binding to the hACE2 receptor and neutralizing *in vitro* infectivity of S-pseudotyped virus and wild-type SARS-CoV-2. All non-human primates (NHPs)

CellPress
OPEN ACCESS

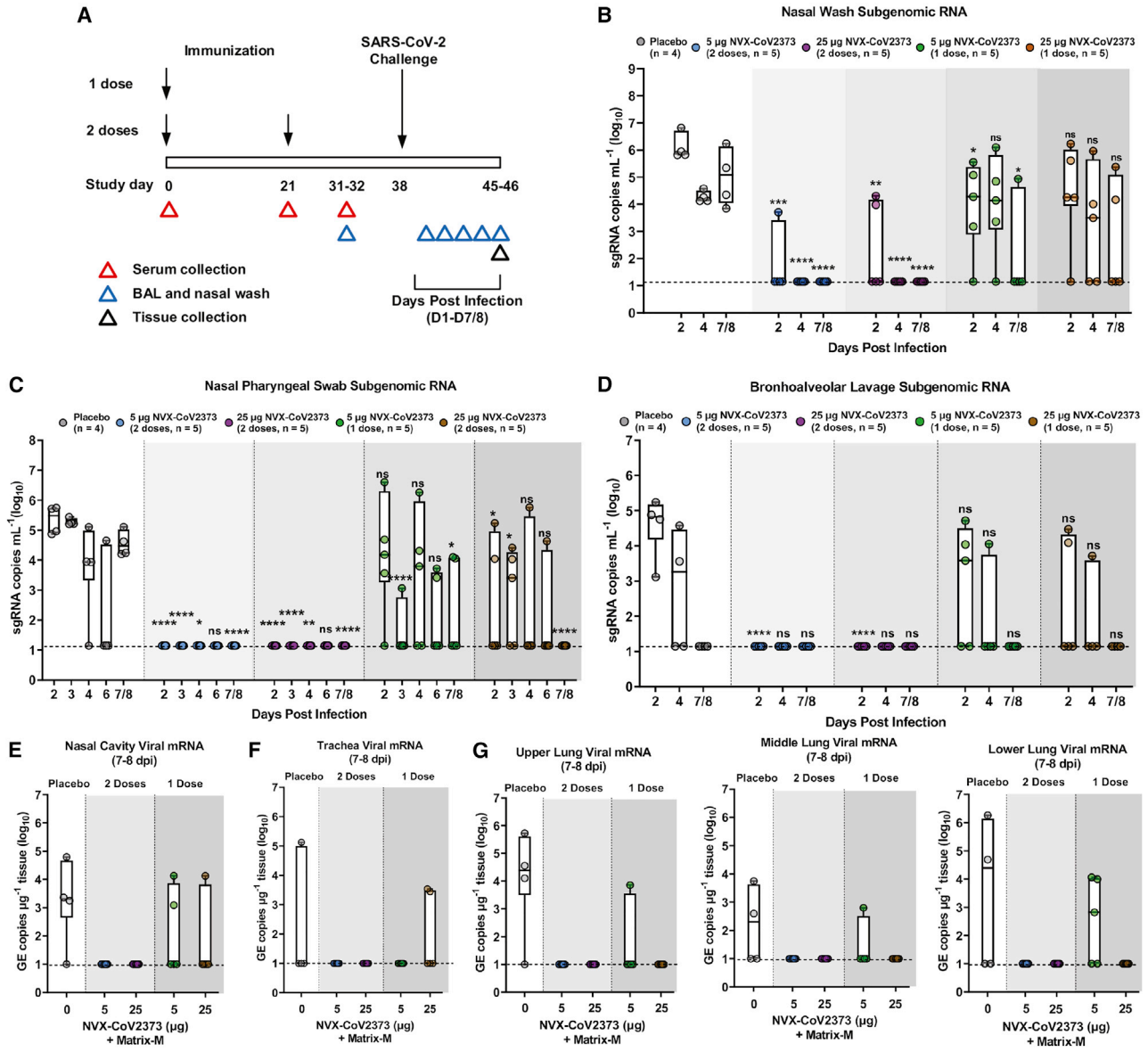

Figure 1. Subgenomic RNA and viral RNA in upper and lower respiratory tract of NVX-CoV2373 immunized rhesus macaques

(A) Groups of adult rhesus macaques (n = 4–5/group) were immunized with a single priming dose (study day 0) or a prime/boost regimen (study days 0 and 21) of 5 μg or 25 μg of NVX-CoV2373 with 50-μg of the Matrix-M adjuvant (0.5 mL; intramuscular [IM]). A separate group (n = 4) received formulation buffer (placebo). Immunized and placebo animals were transferred to an animal biosafety level 3 (ABSL-3) containment facility (study day 31/32) and acclimated for 7 days before challenge with a total of 1.05×10^6 plaque-forming units (pfu) of SARS-CoV-2 (USA-WA1/2020 isolate) in 500 μL, divided between the intranasal (IN) and intratracheal (IT) routes. Animals were monitored daily for up to 7/8 days post-infection (1–7/8 dpi). Serum sample collection days are indicated by the red triangles. Bronchoalveolar lavage (BAL) sample collection days are indicated by the blue triangles. Necropsy and tissue collection is indicated by the black triangle. Quantitative RT-PCR was used to measure the replicating subgenomic (sg) envelope (E) RNA in nasal washes, nasopharyngeal swabs, and BAL samples collected for up to 7–8 dpi.

(B) Nasal washes.

(C) Nasopharyngeal swabs.

(D) BAL aspirates.

(E) SARS-CoV-2 gRNA virus load in the nasal cavity.

(F) Trachea virus load.

(G) Upper, middle, and lower lobes of the lungs of immunized and placebo-treated animals.

In the bar-and-whisker plots, the median is indicated by a horizontal line, the top and bottom of the box indicate the interquartile ranges, and the whiskers indicate the minimum and maximum values. Individual animal values are indicated by the colored symbols. Dashed horizontal lines indicate the limits of detection (LODs). GE copies mL^{-1}, genomic equivalent copies. Significant differences between the placebo group and the immunized groups were determined by the Student's t test (two-tailed, unpaired). ns, not significant, *$p \leq 0.05$, **$p \leq 0.01$, ***$p \leq 0.001$, ****$p \leq 0.0001$.

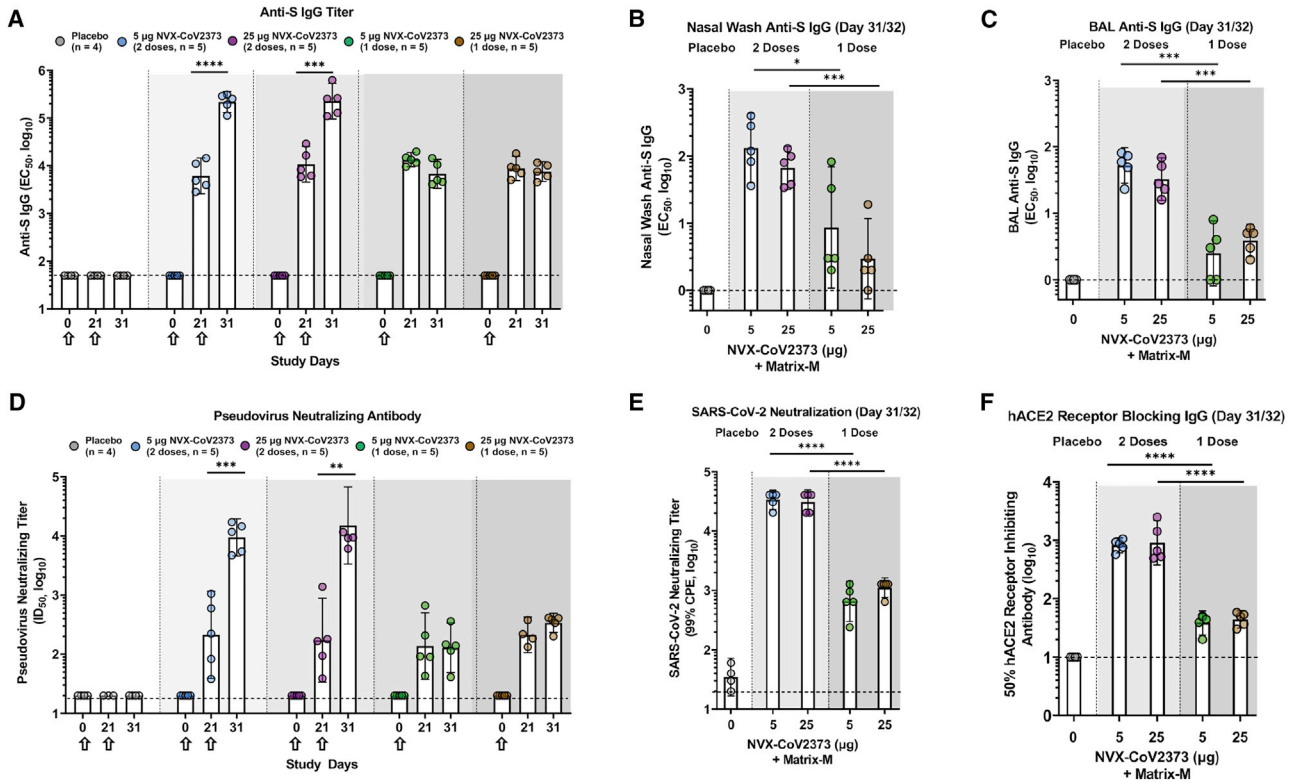

Figure 2. Immunogenicity of NVX-CoV2373 vaccine in rhesus macaques

(A–C) Serum anti-spike (S) IgG titer (A), nasal wash (B), and bronchoalveolar lavage (BAL) (C) samples were collected 31/32 days after the first immunization and before challenge and analyzed for S-specific mucosal IgG (n = 4–5/group).

(D) Pseudovirus-neutralizing titer (ID_{50}).

(E) SARS-CoV-2 neutralizing-antibody titer (99% inhibition of cytopathic effect [99% CPE]) study day 31/32.

(F) hACE2 receptor-blocking antibody titer (study day 31/32).

The geometric mean titers (GMTs) are indicated by the white bars. Hollow arrows indicate prime/boosting with NVX-CoV2373. The error bars indicate the 95% confidence interval (95% CI). Individual animal values are indicated by colored symbols. A Student's t test (unpaired, two-tailed) was used to compare antibody levels between groups immunized with one and two doses. *$p \leq 0.05$, **$p \leq 0.01$, ***$p \leq 0.001$, ****$p \leq 0.0001$. The horizontal dashed lines indicate the LODs for each assay.

treated with one dose had similar neutralization titers, but only some were protected from viral infection, suggesting that neutralization may not be sufficient to fully explain complete protection from infection, particularly after a single vaccine dose.

System serology profiling

Natural SARS-CoV-2 infection is marked by a rapid rise of multiple antibody isotypes and subclasses, each positioned to recruit a diverse set of antibody-effector functions.[16,17] Recent studies have noted a significant correlation between antibody-effector function, rather than neutralization, with natural resolution of infection in humans.[17–19] Thus, we next examined the evolution of subclass, isotype, Fc-receptor (FcR), and Fc-effector function across doses and boosting strategies.

As expected, based on titers (Figure 2), Luminex IgG1 levels were robustly induced after a single vaccine dose, indistinguishably across antigen levels, with a 1.5–4-fold increase after a boost (Figure 3A). Similarly, IgA were induced robustly to a maximal level after one 25-μg dose but required boosting to reach maximal levels in the 5-μg vaccine group (Figure 3A). Conversely, a trend toward higher levels of IgM were noted in the 5-μg vaccine group after a single vaccine dose, which declined with a boost and were largely lost in the 25-μg dose group (Figure 3A), pointing toward enhanced class switching to more-mature antibody subclasses with boosting and higher antigen doses. These data point to the first differences across antigen-dosing group, highlighting equivalent IgG and IgA selection across groups, but more-aggressive switching of IgM, shifting the polyclonal balance of the vaccine-specific antibody pool toward a more-mature Fc-functional profile.

Changes in polyclonal antibody profiles result in the potential formation of distinct swarms of antibodies able to engage with a target pathogen, forming qualitatively distinct immune complexes, which, collectively, shape the FcRs bound on innate immune cells, thereby driving distinct antibody-effector functions.[20–23] The balance and cell expression of activating Fc (FcγRIA, FcγRIIA, and FcγRIIIA) and inhibitory (FcγRIIB) FcR engagement can alter which effector functions are activated.[24] Thus, to explore differences in functionality across doses and boosting regimens, we next profiled differences in binding

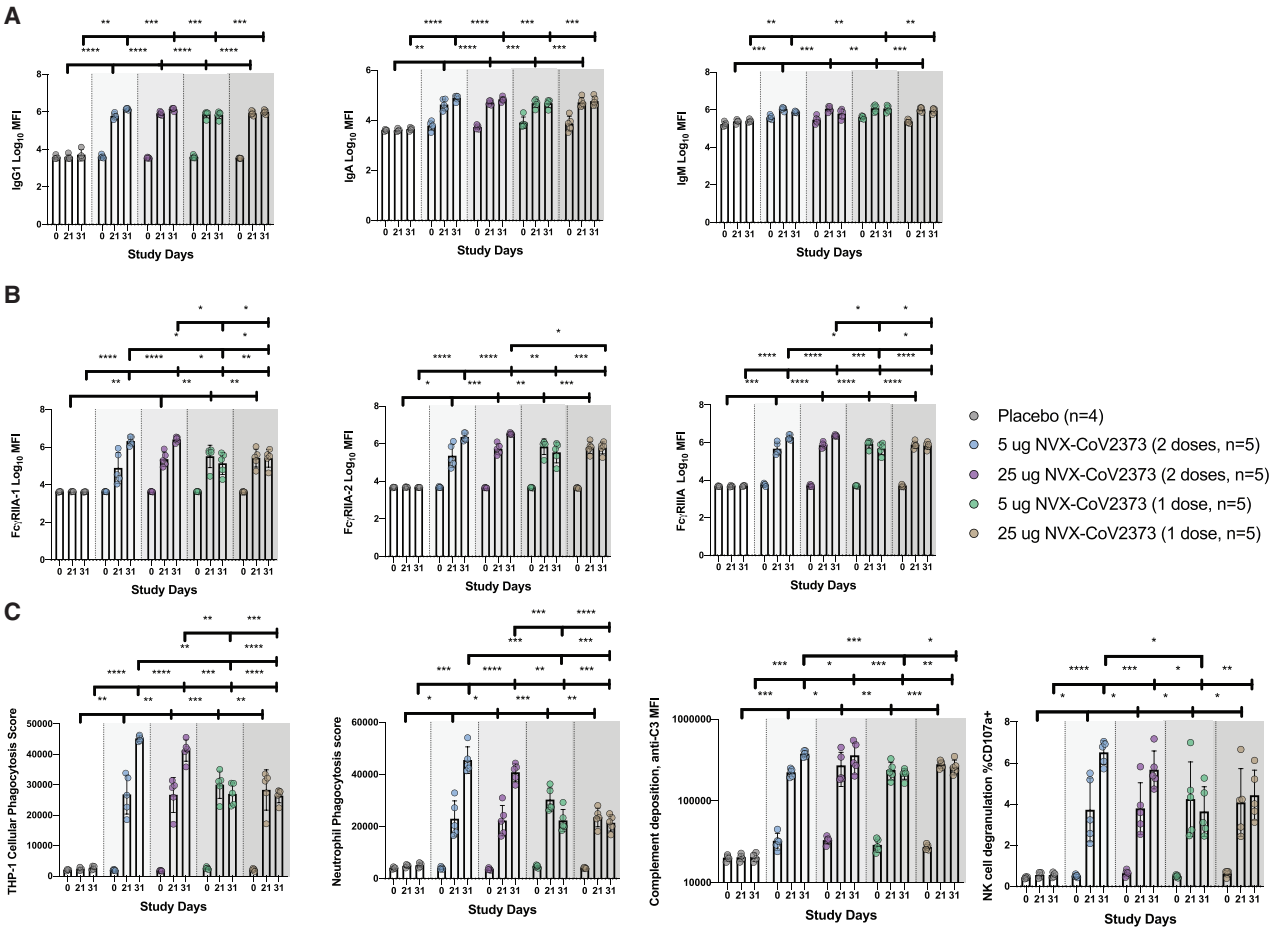

Figure 3. System serology profiling of NVX-CoV2373 immunized rhesus macaques

Serum was collected day 21 and day 31/32 after the first dose of NVX-CoV2373 and was profiled for the anti-NVX-CoV2373 antibody response (n = 4–5/group). (A and B) Luminex was used to quantify the (A) antibody isotypes (IgG1, IgA, and IgM) and (B) FcR binding (FcγRIIA-1, FcγRIIA-2, and FcγRIIIA) for the anti-NVX-CoV2373 antibody response.

(C) The functional anti-NVX-CoV2373-specific antibody responses for antibody-dependent cellular phagocytosis, antibody-dependent neutrophil phagocytosis, antibody-dependent complement deposition, and antibody-dependent NK degranulation (measured by percentage of CD107).

The bars represent the means, and the error bars indicate the SD. Individual animal values are indicated by colored symbols. A two-way ANOVA with Tukey correction for multiple comparisons was used to compare antibody levels between groups. ns, not significant, *p ≤ 0.05, **p ≤ 0.01, ***p ≤ 0.001, ****p ≤ 0.0001.

profiles across activating rhesus FcRs (FcγRIIA-I and FcγRIIIA). Equivalent FcγRIIA-1 binding was observed across the two antigen doses after the prime, although there was a trend to a loss of binding at day 31/32 in the 5-μg dosing group (Figure 3B). However, after a boost, FcγRIIA-1-binding antibodies increased by 4–100-fold across the doses, with a trend toward higher levels of binding antibodies in the 25-μg dosing group (Figure 3B). Nearly identical profiles were observed across the other rhesus FcRs, pointing to a substantial quantitative advantage induced by the boost, which tended to differ across the doses.

Finally, to explore the functional effect of those changes in vaccine-induced antibody Fc profiles, we examined the ability of the humoral response to stimulate antibody-dependent functions: cellular monocyte phagocytosis (ADCP), neutrophil phagocytosis (ADNP), complement deposition (ADCD), and natural killer (NK) degranulation (NKdegran). Similar ADCP responses were induced across the antigen doses after a single vaccination (Figure 3C). Conversely, robust augmentation of ADCP was observed with a boost (Figure 3C), which, surprisingly, tended to be greater in the 5-μg group. An identical profile was observed for NK-cell-activating antibodies. Neutrophil phagocytosis was slightly higher in the 5-μg group after the prime and, then, fully matured across both groups with a boost, remaining slightly elevated in the 5-μg group. Conversely, complement-activating antibodies were induced equivalently across the antigen-dosing groups after a single dose and were increased with a boost in an antigen-dose-independent manner. Thus, although titers and neutralization reached near-maximal potential after a single vaccine dose, those data point to a critical role for boosting in driving the full maturation of the Fc-effector

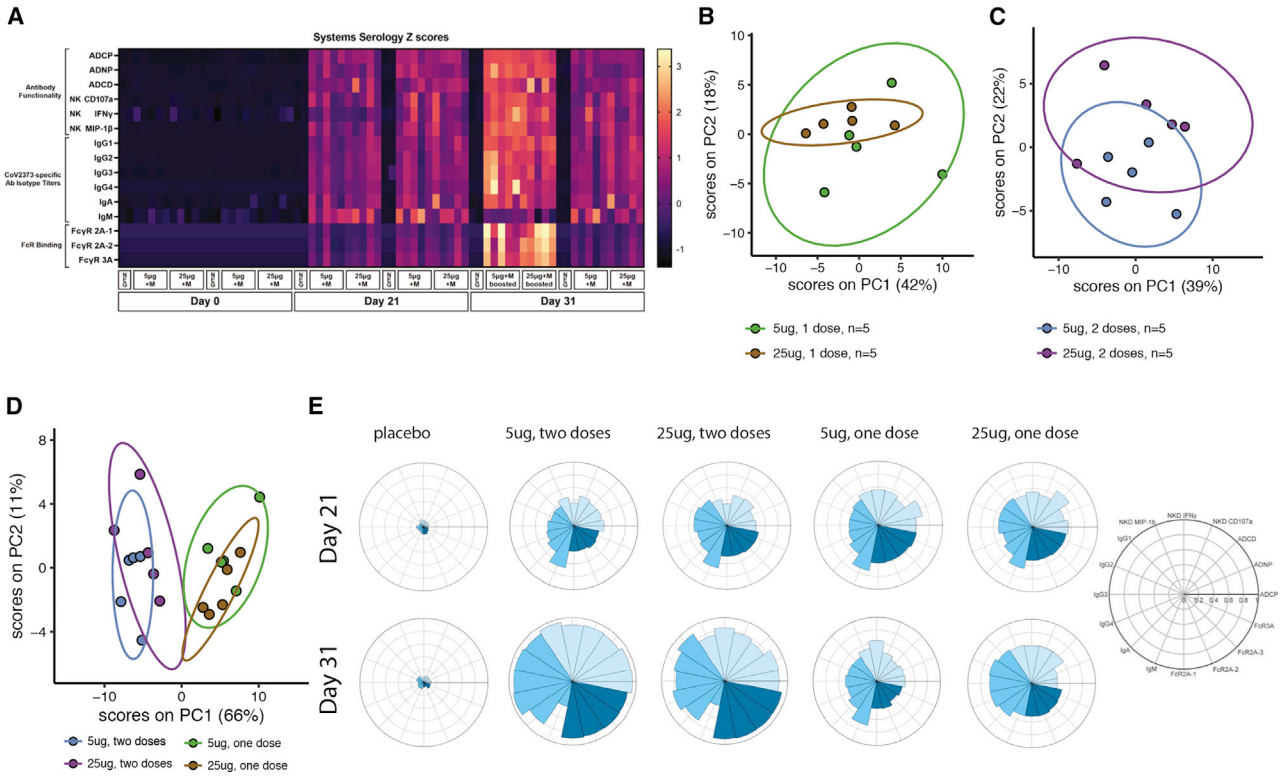

Figure 4. Unique humoral profile of vaccine regimens

Multivariate analysis was performed to distinguish the humoral response between the various vaccine regimens (n = 5/group).

(A) Heatmap of the humoral response to the SARS-CoV-2 spike. Each column is one NHP and one time point. Each row was *Z* scored across itself for the entire cohort.

(B) Principal component analysis (PCA) of antibody features at day 31/32 showing NHPs that received one 5-μg dose (light blue) or one 25-μg dose (dark blue). Ellipses indicate 90% confidence regions assuming a multivariate t distribution.

(C) PCA of antibody features at day 31/32 showing NHPs that received two 5-μg doses (light pink) or two 25-μg doses (dark pink).

(D) PCA of antibody features at day 31/32 showing NHPs that received one 5-μg dose (light pink), one 25-μg dose (dark pink), two 5-μg doses (light blue), or two 25-μg doses (dark blue).

(E) The radar plots show the median percentile for antibody titer, FcR binding, and antibody function (legend on right) for NHPs treated with placebo, two 5-μg doses, two 25-μg doses, one 5-μg dose, or one 25-μg dose in serum collected on day 21 (top row) and day 31/32 (bottom row).

potential of the vaccine-induced humoral response, which is further subtly tuned by antigen dosing.

Unique humoral profiles of the vaccine regimen

Given the various univariate profile differences noted across the vaccine groups, we next aimed to define whether distinct multivariate profiles were induced across the regimens. Aggregate data clearly highlighted the striking influence of the boost and the more-nuanced effects of antigen dose on shaping the polyclonal vaccine response (Figure 4A). Antigen-dose effects emerged upon unsupervised analysis using a principal component analysis (PCA), pointing toward a tendency to separation between antigen dose and vaccine-specific antibody profiles in the animals that received a single dose (Figure 4B), which was largely lost with the boost (Figure 4C). However, integration of the four groups clearly demonstrated the dominant influence of the boost in shaping antibody profiles (Figure 4D). Specifically, robust separation in antibody profiles across single- and double-immunized animal-vaccine-specific antibody profiles (Figure 4D), with a more-subtle effect of dose on shaping vaccine-specific antibody profiles, was observed solely in the single-dose arms. Finally, radar plots of the humoral immune response across vaccine arms demonstrated the clear explosion of humoral immune maturation with the second dose; albeit, slight differences in antibody effector functions were noted across the doses. In addition, more-nuanced differences were observed in the single-dose arms, with a more-balanced functional response observed in the 25-μg group compared with that of the 5-μg immunized animals at days 31–32 before challenge (Figure 4E). These data provide a deep immunologic view of the vaccine-induced polyclonal functional profiles induced after vaccination and how they are shaped by dose and boosting before challenge.

Immune correlates of protection from viral infection

Although neutralizing antibodies have been clearly linked to vaccine-mediated protection after DNA-,[14] AD26-,[13] protein-,[25] and mRNA-based vaccination,[5–7] protection has been noted in

humans before the evolution of neutralizing antibodies.[11,12] Similarly, despite robust induction of neutralizing antibodies given one or two doses of NVX-CoV2373, variable levels of protection were observed against upper and lower respiratory viral loads across the groups (Figures 1B–1G). To define the humoral correlates of immunity of viral control across the respiratory tract, all antibody metrics were integrated, and an unsupervised multivariate analysis was performed to objectively define antibody correlates of immunity. Unsupervised multivariate analysis was performed because of the inherent amplification signal in neutralization assays, which provide a broader dynamic range compared with Fc-effector assays, preventing direct comparison of fold changes across antibody functions. Clear separation was noted in vaccine-induced antibody profiles across NHPs exhibiting complete protection against SARS-CoV-2 compared with animals that exhibited viral loads in two or three compartments (Figure 5A). However, animals that exhibited viral loads in one compartment, exhibited intermediate profiles and were intermingled between both groups. Specifically, the PCA illustrated a substantial split in antibody profiles in animals that exhibited no protection/protection in the lower respiratory tract (BAL) from animals that exhibited more-complete protection across the upper and lower-respiratory tract (nasal washes, nasopharyngeal swabs, and BAL). Thus, unsupervised analysis suggested the presence of unique humoral immune correlates of immunity in the lower and upper respiratory tracts.

To gain deeper resolution into the specific features of the humoral immune response that may lead to these distinct levels of viral restriction across compartments, the relationship of individual features and protection was assessed by calculating the area under the curve for each receiver operator characteristic (ROC) curve within each compartment (Figure 5B). The top features associated with protection in the lower respiratory tract (BAL) included antibody titers, S2- and S1-specific FcR binding, and hACE2 receptor inhibition. Similarly, the top features associated with protection in the BAL and nasopharyngeal swab included the levels of S1-specific antibody titers of several IgG subclasses and hACE2 inhibition. However, complete protection from viral replication across the upper and lower respiratory tracts was associated with a robust whole S-specific multi-subclass-specific response, complement-depositing functions, and neutralizing-antibody titers. These data suggest that specific Fab and Fc functional combinations are necessary to protect across the respiratory tract. The radar plots further illustrated the magnitude and multivariate nature of the protective humoral immune response, marked by poor antibody responses in unprotected animals, an expansion of subclasses, but not functions, in animals with solely lower respiratory tract protection (BAL), an expanded functional and FcR-binding antibody profiles in animals with BAL and nasopharyngeal swab protection. Conversely, the largest, functionally expanded humoral immune response was observed in animals with complete protection across the upper and lower respiratory tract (Figure 5C). These data point the importance of Fc and Fab in driving full viral protection, where neutralization may be key to lower-respiratory protection, but the potential need for additional Fc-effector functions in collaboration with neutralization may be key for full protection across the respiratory tract.

System serology profiling of the human antibody response to NVX-COV2373 and emerging SARS-CoV-2 variants

To finally define whether similar functional humoral profiles are elicited in humans, we deeply profiled humoral immune responses in a phase-1 NVX-CoV2373 study.[25] Antibody profiles were assessed in 79 individuals immunized with NVX-CoV2373, prime and boosted with 25 μg of protein, or prime and boosted with 25 μg and 5 μg of NVX-CoV2373 with the Matrix-M adjuvant (Figure 6A). Globally enhanced humoral immune responses were observed in individuals who received NVX-CoV2373 with the Matrix-M adjuvant (Figure 6B). Moreover, although the differences were small, some separation was observed in the antibody profiles elicited in the 5 and 25 μg adjuvanted dose groups (Figure 6C). Specifically, the adjuvanted 5-μg regimen tended to induce higher antibody titers, FcR-binding titers, and complement functions compared with the 25-μg group (Figure 6D). Conversely, the adjuvanted 25-μg dose group exhibited greater phagocytosis (Figure 6D). Longitudinal profiling of the humoral immune response pointed to only a minor decrease in the immune response between day 49 and day 105 in the 5-μg+Matrix-M immunization, suggesting the vaccine response is capable of inducing a durable and protective immunity (Figure 6E).

Several SARS-CoV-2 variants of concern (VOCs) have been detected across the globe;[26–29] some of which (B.1.1.7) mildly affect neutralizing-antibody responses,[30–32] whereas others (B.1.351) significantly drive neutralization escape.[33–35] In parallel, recent unblinding of global Novavax efficacy data point to robust protection against the B.1.1.7 variant (originally identified in the United Kingdom); however, protection declines to ~60% in South Africa, where the B.1.351 variant was first identified.[34] Given the profound loss of neutralization with the B.1.351 variant, we next aimed to define whether any differences in antibody binding and function could explain differences in observed protection across the VOCs. Thus, we profiled the functional antibody response to the N501Y and Δ69-70 double-mutant (mutations found in B.1.1.7) S (dominant in the UK at the time of the study) and the E484K mutant (mutation found in B.1.351) S (dominant at the time of the South African study) variants compared with the D614G viral variant, the dominant circulating strain.[36] Strong correlations were observed at days 49 and 105 between IgG1 and IgG3 binding levels across the wild-type D614G variant and the two emerging, mutated spikes (Figure 6F). Conversely, some separation was observed across the variants with respect to FcR binding (Figure 6G). Specifically, robust N501YΔ69-70-binding-antibody interactions with FcγR2a and FcγR3a were observed across most Novavax-immunized individuals. However, compromised E484K-binding interactions were noted for both FcRs, with compromised binding to both FcγR2a and FcγR3a in vaccinees who possessed lower antibody titers. Strikingly, vaccinees with high antibody titers bound more efficiently to both FcRs. These data suggest to the following: (1) a disconnect between antibody titers and FcR-binding capabilities, (2) the presence of robust N501YΔ69-70 FcR-binding antibodies, and (3) compromised E484K FcR binding in approximately half of the vaccinees who elicited

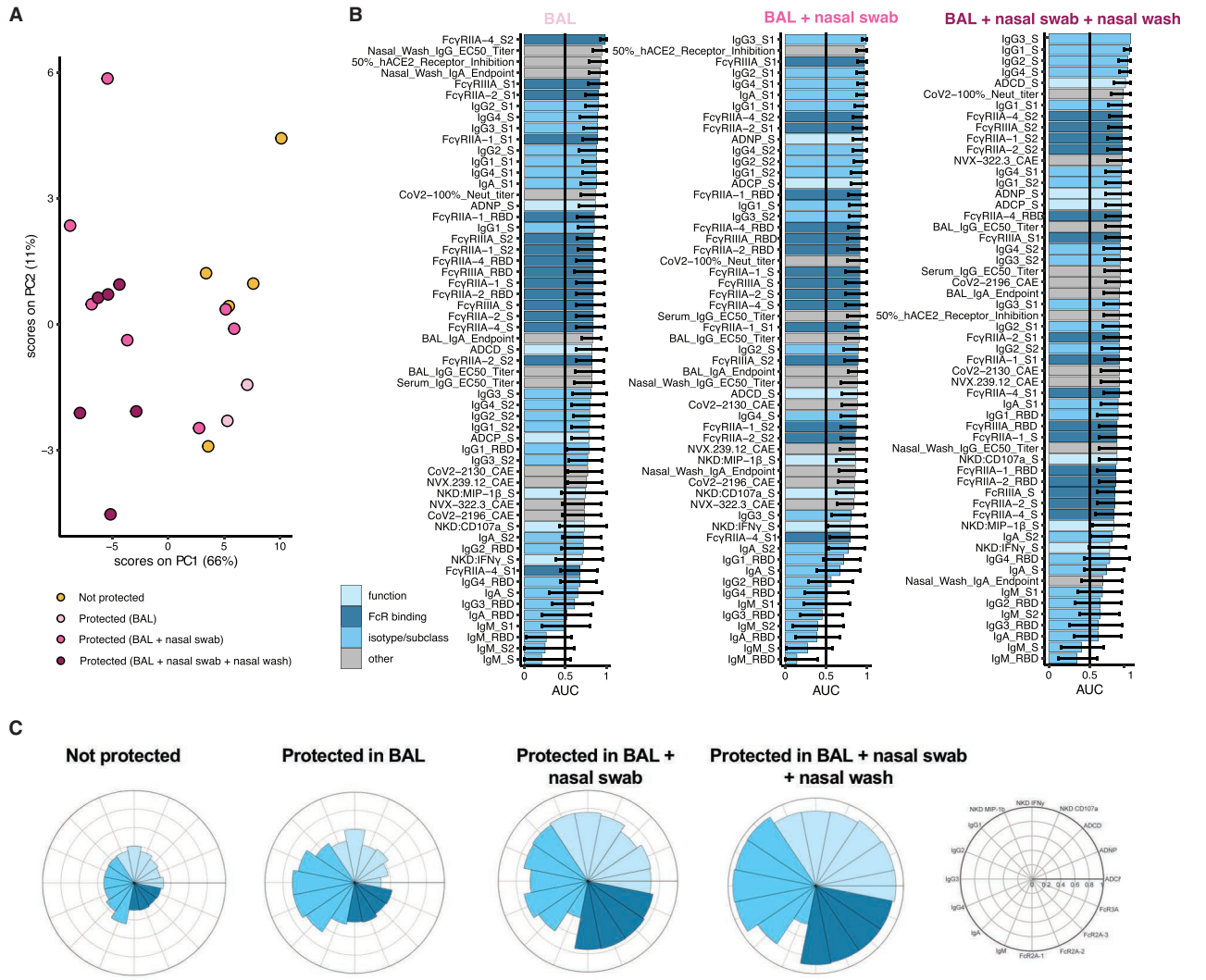

Figure 5. Immune correlates of protection from viral replication

Multivariate analysis was performed to identify the features of a protective humoral response.

(A) PCA for the immunized NHPs (n = 20, no placebos included) indicating protected (blue) NHPs with no detectable virus in BAL, BAL + nasopharyngeal swab, BAL + nasopharyngeal swab + nasal wash versus non-protected (yellow) NHPs. Ellipses indicate 90% confidence regions, assuming a multivariate t distribution, and are shown for protected and non-protected NHPs.

(B) Correlates of protection for BAL (n = 20), nasopharyngeal swab (n = 20), or nasal wash (n = 19) at day 31/32. The area under the curve (AUC) for the receiver operator characteristic (ROC) curve is shown. Error bars indicate the 95% confidence intervals (95% CI) for each antibody feature.

(C) The radar plots show the median percentile for antibody titer, FcR binding, and antibody function (legend on right) for non-protected, protected in BAL, protected in BAL + nasopharyngeal swab, or protected in BAL + nasopharyngeal swab + nasal wash NHPs.

lower antibody titers. These data closely mimic efficacy results pointing to robust protection against N501YΔ69-70 but compromised protection against the E484K variant consistent with FcR binding in roughly half of high-titer vaccinees. This suggests that, although there may be some decline in FcR binding in individuals who mount high vaccine titers, that reduction is less pronounced than the reduction observed in neutralization, particularly among individuals with high levels of vaccine-induced binding antibodies that bind and recognize VOCs. Conversely, individuals with low or intermediate vaccine-titers exhibit highly compromised FcR binding and reduced neutralizing-antibody responses collectively, resulting in poor protection against infection. These data highlight the importance of examining antibody functions beyond neutralization as potential mechanistic correlates of immunity against VOCs. Thus, FcR-binding activity may compensate for a loss of neutralization, providing continued protection from disease in a complementary manner to neutralization, supporting the observation of Fab and Fc cooperation to drive maximal protection against SARS-CoV-2.

CellPress
OPEN ACCESS

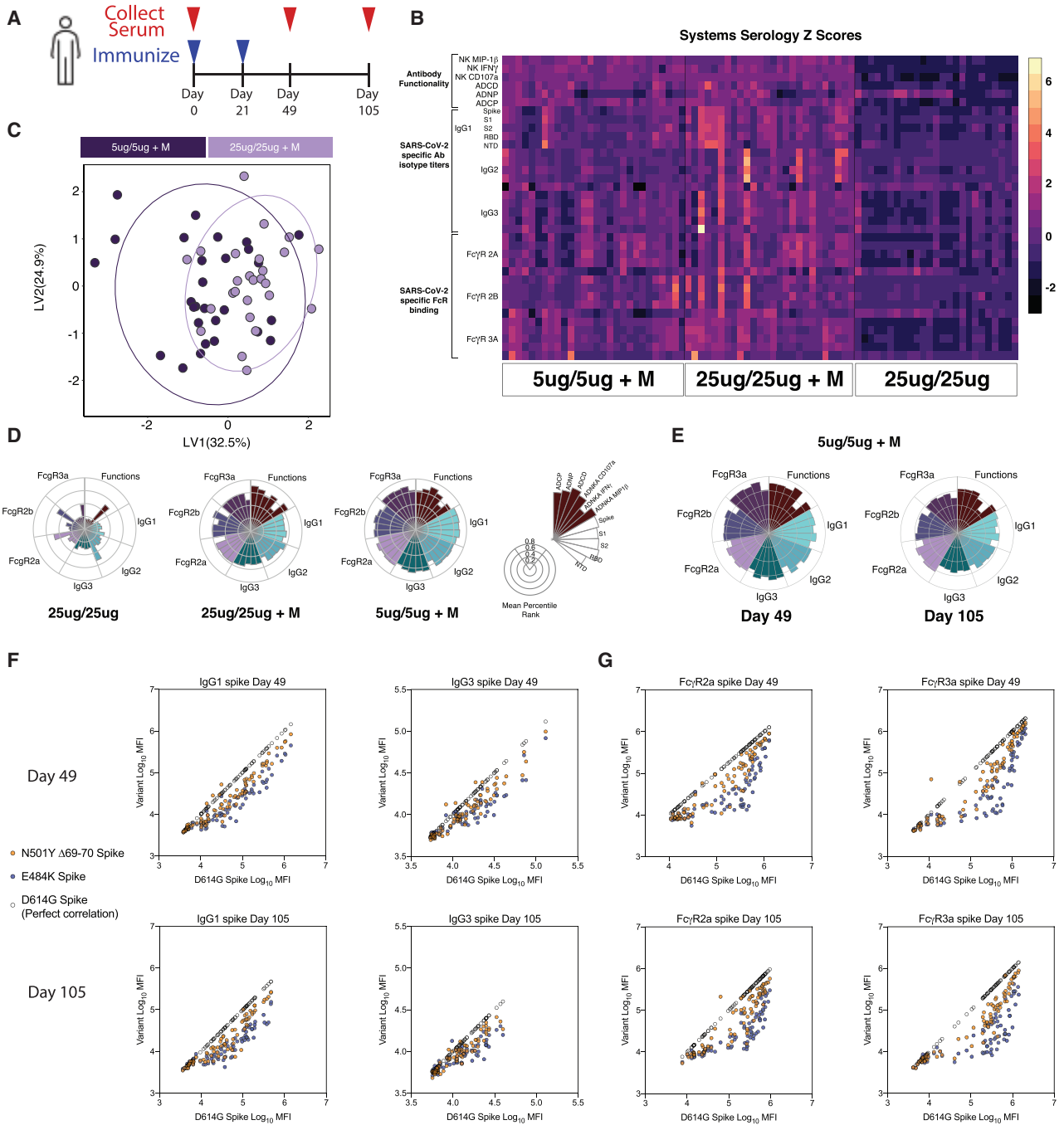

Figure 6. Antibody binding and functionality of human vaccine response against WT and variant SARS-CoV-2

(A) Humans were vaccinated with 25 μg or 5 μg of NVX-CoV2373 with or without adjuvant on days 0 and 21, and serum was collected days 0, 49, and 105; 25 μg/25 μg, n = 25; 25 μg/25 μg + M, n = 26; 5 μg/5 μg + M, n = 28.

(B) Heatmap of the humoral response to SARS-CoV-2 spike, S1, S2, receptor-binding domain, and N-terminal domain protein on day 49. Luminex was used to quantify the antibody isotypes (IgG1, IgG2, and IgG3) and FcR (FcγRIIA, FcγRIIB, and FcγRIIIA) binding profiles. Functional responses were quantified against Spike protein. Each column represents an individual, and each row represents one humoral feature *Z* scored across the row.

(C) Partial least-squares discriminant analysis (PLS-DA) plot depicts the multivariate antibody profiles classified by dose in vaccine + adjuvant immunized individuals on day 49. The mean AUC score after 100 trials of 5-fold cross-validation is 0.75.

(D) The nightingale rose plots show the median percentile for antibody titer, FcR binding, and antibody function (legend on right) for humans immunized with 25 μg or 5 μg of NVX-CoV2373 with or without adjuvant on day 49.

(legend continued on next page)

DISCUSSION

Vaccine shortages, the need for rapid global deployment, increasing reinfection cases, and the emergence of VOCs have collectively pointed to the urgent need to define correlates of immunity against SARS-CoV-2 and its variants. With the growing global shift toward the use of a single dose of mRNA or using delayed boosting to achieve population-level immunity,[37–39] along with the single Ad26 dose vaccine, as well as the eminent decline in antibody titers with inevitable vaccine waning, defining antibody correlates of protection induced across doses and antibody titers is needed urgently. Using a unique vaccine study, poised to profile both the importance of antigen dose and boosting, here, we deeply and comprehensively dissected the key correlates of humoral immunity against upper and lower respiratory tract infection. Despite the induction of robust vaccine-specific antibody titers and neutralization with a single dose or two doses of 5-μg or 25-μg NVX-CoV2373, differential levels of viral restriction were observed across animals in the upper and lower respiratory tracts. Specifically, animals receiving a single-dose vaccine were only partially protected against replicating virus in the upper respiratory tract, whereas animals receiving two doses exhibited near-complete protection. These data suggest that a single dose may prevent disease, but that two doses may be essential to block further transmission.

The improved protection of the two-dose vaccine was linked to a dramatic maturation of the Fc-effector profiles of vaccine-induced antibodies, which collaborated with neutralization as key correlates of immunity against viral replication, with highly functional and neutralizing-antibody responses conferring the most-robust restriction across the upper and lower respiratory tract. Thus, overall, these data demonstrate the critical importance of a coordinated Fab- and Fc-mediated antibody response for full protection against SARS-CoV-2 infection, which may also function against emerging variants. These data agree with several recent studies showing neutralizing monoclonal antibodies require Fc-effector function for optimal protection in animal models and are in line with the observed induction of antibody-effector functions and neutralizing antibodies that track with protection after SARS-CoV-2 vaccination in humans.[40–45]

Both human mRNA vaccines—mRNA-1273 and BNT162b2—require a prime and a boost to achieve optimal protection. However, as the logistical challenges become apparent in distributing a vaccine globally, interest in increasing the available vaccine by reducing the amount of vaccine or doses given per individual has increased. Preliminary retrospective analysis of the first dose of the Pfizer/BNT162b2 before boosting suggested approximately a 52% protection from severe infection, whereas more-recent studies have suggested a single dose is 85% effective at preventing death.[5,46,47] In addition, recent results from Johnson and Johnson's single-dose adenovirus vaccine, Ad26.COV2.S, has demonstrated 66% efficacy against moderate and severe COVID-19,[48] and results from AstraZeneca demonstrated an ~80% efficacy at preventing hospitalization with a single-dose of ChAdOx1.[47] However, whether a single dose can provide long-term protection remains unclear. Although immunogenicity and durability vary significantly across vaccine platforms,[5–7,13,14,25] our data demonstrate some level of protection against lower-respiratory infection after a single vaccine. However, single-dose vaccine-maintained IgM exhibited incomplete class switching, poor mucosal antibody levels, and incomplete functional effector and neutralizing responses, albeit a more-balanced response was noted at the higher (25 μg) antigen dose. However, after two doses at 5 μg or 25 μg, the explosion of antibody effector function and neutralization likely resulted in a significant increase in protection against both upper and lower respiratory viral replication, linked to the combined presence of potent neutralizing and Fc-effector-inducing antibodies and continues to point to the value of the booster immunization. Our data argue that, although a single dose of antibody may not block transmission, antibodies induced after a single dose with the capability to neutralize and drive antibody-effector function, collectively contribute to antiviral control; however, further research is necessary to confirm these observations in humans. Moreover, the significant loss of neutralization with VOCs, despite continued protection from severe disease and death in South Africa, points to the potential, critical importance of antibody-effector function against variants. Thus, ongoing breakthrough-correlate analyses will define the compensatory contribution of Fc-effector function to protection against VOCs.

Neutralizing antibodies represent a critical obstacle to viral infection at the time of infection. However, the density of antibody-producing cells and innate cells likely varies along the respiratory tract.[49–53] Thus, to achieve complete sterilizing protection from infection in the upper respiratory tract, it is plausible that additional immune mechanisms may be required in the upper respiratory tract to compensate for potentially lower antibody levels. Here, we observed the key role of neutralizing antibodies deep within the lungs, but the critical importance of SARS-CoV-2 antibodies of multiple subclasses, binding to multiple FcRs, and complement activation as key additional functional mechanisms that may contribute to upper respiratory protection. Given that the NVX-CoV2373 vaccine induced potent neutralizing antibodies across doses and regimens, we were unable to divorce the influence of neutralization and Fc-effector function. Similar profiles have been noted after reinfection, DNA, and Ad26-vaccine studies, marking the co-evolution of the Fab and Fc, and the importance of both ends of the molecule in protective immunity.[13,14] However, knowing whether neutralization and/or Fc-effector function persist differentially over time after vaccination may provide key insights on precise, durable correlates of immunity.

Because the virus has begun to adapt to populations across the globe, a number of SARS-CoV-2 VOCs have begun to

(E) The nightingale rose plots show the median for antibody titer, FcR binding, and antibody function (legend on right) for humans immunized with 5 μg of NVX-CoV2373 + Matrix-M adjuvant on days 49 and 105.

(F and G) Luminex was used to quantify the antibody isotypes (IgG1 and IgG3) (F) and FcR binding (FcγRIIA and FcγRIIIA) (G) to the dominant circulating strain (D614G) and to variant N501YΔ69-70 (mutations found in B.1.1.7) and E484K (mutation found in B.1.351) SARS-CoV-2 spike proteins. D614G spike is correlated to itself, generating a perfect correlation (clear circle) to provide a visual reference for theoretically equivalent binding.

emerge. The D641G mutation spread rapidly from Europe to other continents, resulting in a conformational change in the rigidity of the receptor-binding domain (RBD), resulting in enhanced infectivity *in vitro*, but resulting in no escape from neutralizing antibodies.[36,54–57] Similarly, recently, the B.1.1.7 mutation has spread across and out of the UK, since September 2020,[27] representing three key mutations—N501Y, P681H, and Δ69-70—which have been linked to enhanced ACE2 binding but limited effect on neutralizing-antibody activity by the monoclonal or Pfizer/BNT162b2 vaccine.[26,31,32,58–61] Additional variants have begun to emerge in South Africa (B.1.351/501Y.V2) and Brazil (P.1), including mutations both in the RBD and in the N-terminal domain of the S-protein, demonstrating significant evasion of antibody-mediated neutralization.[32,60–68] Here, we noted a loss of antibody FcR-binding activity to the E484K S, particularly in vaccinees with low vaccine titers, but more-persistent antibody-mediated FcR binding to the N501YΔ69-70 S. These data mirror the rates of protection observed in the recent phase 2b and 3 vaccine studies, wherein NVX-CoV2373 was 89% effective in the UK (where the B1.1.7 variant dominated at the time of the study) but <60% effective in South Africa (where the B1.351 variant dominated at the time of the study),[34,35] further substantiating the potential critical importance of the collaboration between the Fab and Fc functionality in overall population-level vaccine efficacy, even in the setting of a loss of neutralization. Surprisingly, a third of patients enrolled in the South Africa clinical trial were seropositive before enrollment, with nearly equivalent rates of infection in the placebo arm among COVID-19 convalescents and naive volunteers.[35] These data argue that prior infection may not provide protection from subsequent infections with SARS-CoV-2 variants, further illustrating the necessity of vaccines. However, further research is needed to dissect the mechanistic contribution of vaccine-induced Fab and Fc to control and to clear all SARS-CoV-2 variants.

As the need to develop new vaccines, treatments, and adjuvants increases for additional pathogens, beyond SARS-CoV-2, the ability to translate from animal models to human immunity remains critical. Using the same vaccine, adjuvant, and similar doses to immunize NHPs and humans allowed us to demonstrate the similarity in the immune response across the species. Similar to natural correlates of immunity after COVID-19 infection in humans,[17,18] NVX-CoV2373-immunized NHPs that were protected had high anti-spike titers and opsonophagocytic functions after immunizations, suggesting that NVX-CoV2373 can induce a protective response similar to that observed with natural resolution of disease. Furthermore, the 5-μg two-dose regimen induced a slightly higher immune response in both NHPs and humans, highlighting the utility of the NHP model for dose selection. All together, these data demonstrate the ability of the rhesus macaque model to predict human vaccine responses, highlighting the importance of this model for the design of new vaccines and treatments for SARS-CoV-2 and beyond.

After just 4 months, the World Health Organization (WHO) declared that the SARS-CoV-2 virus had caused a worldwide pandemic. In response, several vaccines have progressed through late stages of clinical evaluation. To date, the BNT162b2 vaccine has been licensed, and the mRNA-1273 vaccine has received Emergency Use Authorization (EUA). Although these vaccines have an acceptable safety profile and effectively protect against more-severe disease, they require freezing, have limited data on long-term durability, and have not been shown to protect against infection or transmission. Moreover, given the few vaccine doses available, additional vaccine candidates that are able to counteract both wild-type and emerging variant strains are urgently needed. Thus, the need to understand correlates of immunity has never been more urgent, to support the selection and design of additional vaccines able to confer global protective immunity. Here, we describe the identification of correlates of immunity using a subunit vaccine that is stable at refrigerated temperatures and is immunogenic and well tolerated in human studies.[25] In this study, we demonstrate the presence of binding and neutralizing-antibody titers after a single immunization dose, using either 5 μg or 25 μg of the vaccine, but a remarkable maturation of the Fc-effector profile after a second immunization. Moreover, although partial protection was observed with neutralizing antibodies alone after a single round of immunization, complete protection in the upper and lower respiratory tract was observed with a second round of immunization, marking critical Fab- and Fc-mediated correlates of immunity, which may be key to both protection against disease and transmission of SARS-CoV-2 and emerging VOCs. Likewise, robust protection was observed against the B1.1.7 VOC,[34] to which neutralization and FcR function was robust. Conversely although emerging data suggest compromised neutralization against the B1.351 VOC,[26,69] FcR binding was preserved in roughly more than half of the individuals that elicited high antibody titers, roughly the number of individuals that were ultimately protected from infection in the phase 2b trial.[34] Thus, collectively, these data support the critical collaborative function of the Fab and Fc toward achieving maximal protection across respiratory compartments and across emerging VOCs, providing key insights into the mechanisms that may be essential to achieve global immunity against SARS-CoV-2.[70,71]

LIMITATIONS OF STUDY

Although our study was limited to n = 4–5 NHPs per treatment group, those numbers were powered to detect infectious-outcome signals and to adhere to standards in SARS-CoV-2 NHP studies.[13,15,72,73] Larger animal studies could identify additional differences across the groups, but even with these small numbers, significant univariate and multivariate differences were observed. Moreover, given the co-induction of Fc-effector function and neutralization, in this study, we were unable to quantify the exact contribution of each function in protection against SARS-CoV-2. However, emerging studies using heterologous wild-type vaccination and VOC challenge have begun to probe the importance of both Fc-effector function and T cell immunity in the setting of reduced neutralization.[74,75] Linked to previous studies, which have demonstrated that both neutralization and Fc-mediated functions are necessary in monoclonal treatments,[43] future studies are likely to unlock the precise role of each antibody domain in the mechanism of control against SARS-CoV-2.

STAR★METHODS

Detailed methods are provided in the online version of this paper and include the following:

- KEY RESOURCES TABLE
- RESOURCE AVAILABILITY
  - Lead contact
  - Materials availability
  - Data and code availability
- EXPERIMENTAL MODEL AND SUBJECT DETAILS
  - Animal studies
  - Human subjects
  - Cell lines
  - Viruses
- METHOD DETAILS
  - Study blinding
  - Study design
  - NVX-CoV2373 spike glycoprotein
  - Anti-spike IgG and IgA ELISA
  - Human angiotensin converting enzyme 2 (hACE2) receptor blocking antibody
  - SARS-CoV-2 neutralizing antibody assay
  - Preparation of the SARS-CoV-2 challenge stock
  - SARS-CoV-2 challenge
  - Sample collection for SARS-CoV-2 RNA quantification
  - Quantification of virus load in nasopharyngeal swabs, nasal washes, BAL, and tissues
  - Antibody-dependent cellular phagocytosis and neutrophil phagocytosis
  - Antibody-dependent complement deposition
  - Antibody-dependent NK cell degranulation
  - Isotype and FcR-binding Luminex profiling
- QUANTIFICATION AND STATISTICAL ANALYSIS
- ADDITIONAL RESOURCES

SUPPLEMENTAL INFORMATION

Supplemental information can be found online at https://doi.org/10.1016/j.xcrm.2021.100405.

ACKNOWLEDGMENTS

This work was funded by Operation Warp Speed. We thank Kathryn Hastie for helpful discussions. We thank Kristal Lam for handling samples and materials for animal studies. We thank Nancy Zimmerman, Mark and Lisa Schwartz, an anonymous donor (financial support), Terry and Susan Ragon, and the SAMANA Kay MGH research scholars award for their support. We acknowledge support from the Ragon Institute of MGH, MIT and Harvard, the Massachusetts Consortium on Pathogen Readiness (MassCPR), the NIH (3R37AI080289-11S1, R01AI146785, U19AI42790-01, U19AI135995-02, U19AI42790-02S1, 1U01CA260476-01, and CIVIC75N93019C00052), National Science Foundation graduate research fellowship grant no. 1745302, the Gates Foundation Global Health Vaccine Accelerator Platform funding (OPP1146996 and INV-001650), the COVID-19 Therapeutics Accelerator (INV-006133), and the Musk Foundation. Research work in the Krammer laboratory was partially funded by the Centers of Excellence for Influenza Research and Surveillance (CEIRS, contract no. HHSN272201400008C); by the generous support of the JPB Foundation and the Open Philanthropy Project (research grant 2020-215611 [5384]); and by anonymous donors. The graphical abstract was created with BioRender.com.

AUTHOR CONTRIBUTIONS

N.P., M.G.-X., Y.G.-G., R.C., J.-H.T., B.Z., M.J.M., A.D.P., M.J.G., C.A., A.L.Z., G.A., C.L., K.M.P., E.O.S., D.L., F.K., and G.S. contributed to conceptualization of experiments, generation of data and analysis, and interpretation of the results. N.P., J.-H.T., B.Z., S.M., Y.G.-G., R.C., C.A., M.J.G., A.L.Z., D.Y., K.A.B., F.A., S.S., M.E.M., J.L., C.M., and M.B.F. performed experiments. N.P., M.G.-X., Y.G.-G., R.C., G.A., and M.B.F. coordinated projects. G.S., G.G., D.L., D.M., M.G.-X., A.M.G., N.P., Y.G.-G., R.C., M.B.F., M.J.G, C.A., G.A., C.L., K.M.P., and L.E. contributed to drafting and making critical revisions with the assistance of others.

DECLARATION OF INTERESTS

N.P., M.G.-X., J.-H.T., B.Z., S.M., A.M.G., M.J.M., A.D.P., G.G., G.S., and L.E. are current or past employees of Novavax, Inc. and have stock options in the company. G.A. is the founder of SeromYx Systems, Inc. A.L.Z. is a current employee of Moderna, Inc. but conducted this work before employment. The Icahn School of Medicine at Mount Sinai has filed patent applications relating to SARS-CoV-2 serological assays and NDV-based SARS-CoV-2 vaccines, which list F.K. as co-inventor. F.A. is also listed on the serological assay patent application as a co-inventor. Mount Sinai has spun out a company, Kantaro, to market serological tests for SARS-CoV-2. F.K. has consulted for Merck and Pfizer (before 2020) and is currently consulting for Pfizer, Seqirus, and Avimex. The Krammer laboratory is also collaborating with Pfizer on animal models of SARS-CoV-2. Any opinion, findings, and conclusions or recommendations expressed in this material are those of the author(s) and do not necessarily reflect the views of the National Science Foundation. Y.G.-G., R.C., M.J.G., C.A., K.M.P., C.L., D.Y., K.A.B., M.E.M., J.L., D.M., C.M., S.S., F.A., E.O.S, D.L., and M.B.F. declare no competing interest.

Received: April 1, 2021
Revised: June 30, 2021
Accepted: August 24, 2021
Published: August 31, 2021

REFERENCES

1. Dong, E., Du, H., and Gardner, L. (2020). An interactive web-based dashboard to track COVID-19 in real time. Lancet Infect. Dis. *20*, 533–534.
2. Huff, H.V., and Singh, A. (2020). Asymptomatic transmission during the coronavirus disease 2019 pandemic and implications for public health strategies. Clin. Infect. Dis. *71*, 2752–2756.
3. Day, M. (2020). Covid-19: identifying and isolating asymptomatic people helped eliminate virus in Italian village. BMJ *368*, m1165.
4. Meng, L., Qiu, H., Wan, L., Ai, Y., Xue, Z., Guo, Q., Deshpande, R., Zhang, L., Meng, J., Tong, C., et al. (2020). Intubation and ventilation amid the COVID-19 outbreak: Wuhan's experience. Anesthesiology *132*, 1317–1332.
5. Polack, F.P., Thomas, S.J., Kitchin, N., Absalon, J., Gurtman, A., Lockhart, S., Perez, J.L., Pérez Marc, G., Moreira, E.D., Zerbini, C., et al.; C4591001 Clinical Trial Group (2020). Safety and efficacy of the BNT162b2 mRNA COVID-19 vaccine. N. Engl. J. Med. *383*, 2603–2615.
6. Jackson, L.A., Anderson, E.J., Rouphael, N.G., Roberts, P.C., Makhene, M., Coler, R.N., McCullough, M.P., Chappell, J.D., Denison, M.R., Stevens, L.J., et al.; mRNA-1273 Study Group (2020). An mRNA vaccine against SARS-CoV-2—preliminary report. N. Engl. J. Med. *383*, 1920–1931.
7. Poland, G.A., Ovsyannikova, I.G., and Kennedy, R.B. (2020). SARS-CoV-2 immunity: review and applications to phase 3 vaccine candidates. Lancet *396*, 1595–1606.
8. Sadoff, J., Le Gars, M., Shukarev, G., Heerwegh, D., Truyers, C., de Groot, A.M., Stoop, J., Tete, S., Van Damme, W., Leroux-Roels, I., et al. (2021). Interim results of a phase 1-2a trial of Ad26.COV2.S COVID-19 vaccine. N. Engl. J. Med. *384*, 1824–1835.

9. Folegatti, P.M., Ewer, K.J., Aley, P.K., Angus, B., Becker, S., Belij-Rammerstorfer, S., Bellamy, D., Bibi, S., Bittaye, M., Clutterbuck, E.A., et al.; Oxford COVID Vaccine Trial Group (2020). Safety and immunogenicity of the ChAdOx1 nCoV-19 vaccine against SARS-CoV-2: a preliminary report of a phase 1/2, single-blind, randomised controlled trial. Lancet *396*, 467–478.

10. Dagan, N., Barda, N., Kepten, E., Miron, O., Perchik, S., Katz, M.A., Hernán, M.A., Lipsitch, M., Reis, B., and Balicer, R.D. (2021). BNT162b2 mRNA COVID-19 vaccine in a nationwide mass vaccination setting. N. Engl. J. Med. *384*, 1412–1423.

11. U.S. Food and Drug Administration (2021). Vaccines and Related Biological Products Advisory Committee meeting. https://www.fda.gov/advisory-committees/vaccines-and-related-biological-products-advisory-committee/2021-meeting-materials-vaccines-and-related-biological-products-advisory-committee.

12. Nature Editors (2021). UK science advisers: publish evidence behind COVID vaccine changes. Nature *589*, 169–170.

13. Mercado, N.B., Zahn, R., Wegmann, F., Loos, C., Chandrashekar, A., Yu, J., Liu, J., Peter, L., McMahan, K., Tostanoski, L.H., et al. (2020). Single-shot Ad26 vaccine protects against SARS-CoV-2 in rhesus macaques. Nature *586*, 583–588.

14. Yu, J., Tostanoski, L.H., Peter, L., Mercado, N.B., McMahan, K., Mahrokhian, S.H., Nkolola, J.P., Liu, J., Li, Z., Chandrashekar, A., et al. (2020). DNA vaccine protection against SARS-CoV-2 in rhesus macaques. Science *369*, 806–811.

15. Guebre-Xabier, M., Patel, N., Tian, J.H., Zhou, B., Maciejewski, S., Lam, K., Portnoff, A.D., Massare, M.J., Frieman, M.B., Piedra, P.A., et al. (2020). NVX-CoV2373 vaccine protects cynomolgus macaque upper and lower airways against SARS-CoV-2 challenge. Vaccine *38*, 7892–7896.

16. Loos, C., Atyeo, C., Fischinger, S., Burke, J., Slein, M.D., Streeck, H., Lauffenburger, D., Ryan, E.T., Charles, R.C., and Alter, G. (2020). Evolution of early SARS-CoV-2 and cross-coronavirus immunity. MSphere *5*, e00622-20.

17. Atyeo, C., Fischinger, S., Zohar, T., Slein, M.D., Burke, J., Loos, C., McCulloch, D.J., Newman, K.L., Wolf, C., Yu, J., et al. (2020). Distinct early serological signatures track with SARS-CoV-2 survival. Immunity *53*, 524–532.e4.

18. Zohar, T., Loos, C., Fischinger, S., Atyeo, C., Wang, C., Slein, M.D., Burke, J., Yu, J., Feldman, J., Hauser, B.M., et al. (2020). Compromised humoral functional evolution tracks with SARS-CoV-2 mortality. Cell *183*, 1508–1519.e12.

19. Brunet-Ratnasingham, E., Anand, S.P., Gantner, P., Moquin-Beaudry, G., Dyachenko, A., Brassard, N., Beaudoin-Bussières, G., Pagliuzza, A., Gasser, R., Benlarbi, M., et al. (2021). Integrated immunovirological profiling validates plasma SARS-CoV-2 RNA as an early predictor of COVID-19 mortality. medRxiv. https://doi.org/10.1101/2021.03.18.21253907.

20. Nimmerjahn, F., and Ravetch, J.V. (2008). Fcγ receptors as regulators of immune responses. Nat. Rev. Immunol. *8*, 34–47.

21. Bournazos, S., and Ravetch, J.V. (2017). Diversification of IgG effector functions. Int. Immunol. *29*, 303–310.

22. Bournazos, S., and Ravetch, J.V. (2015). Fcγ receptor pathways during active and passive immunization. Immunol. Rev. *268*, 88–103.

23. Bournazos, S., Gupta, A., and Ravetch, J.V. (2020). The role of IgG Fc receptors in antibody-dependent enhancement. Nat. Rev. Immunol. *20*, 633–643.

24. Crowley, A.R., and Ackerman, M.E. (2019). Mind the gap: how interspecies variability in IgG and Its receptors may complicate comparisons of human and non-human primate effector function. Front. Immunol. *10*, 697.

25. Keech, C., Albert, G., Cho, I., Robertson, A., Reed, P., Neal, S., Plested, J.S., Zhu, M., Cloney-Clark, S., Zhou, H., et al. (2020). Phase 1–2 trial of a SARS-CoV-2 recombinant spike protein nanoparticle vaccine. N. Engl. J. Med. *383*, 2320–2332.

26. Xie, X., Liu, Y., Liu, J., Zhang, X., Zou, J., Fontes-Garfias, C.R., Xia, H., Swanson, K.A., Cutler, M., Cooper, D., et al. (2021). Neutralization of SARS-CoV-2 spike 69/70 deletion, E484K and N501Y variants by BNT162b2 vaccine-elicited sera. Nat. Med. *27*, 620–621.

27. Kupferschmidt, K. (2020). Mutant coronavirus in the United Kingdom sets off alarms, but its importance remains unclear. Science Magazine, December 20, 2020. https://doi.org/10.1126/science.abg2626. https://www.sciencemag.org/news/2020/12/mutant-coronavirus-united-kingdom-sets-alarms-its-importance-remains-unclear.

28. Kemp, S.A., Collier, D.A., Datir, R.P., Ferreira, I.A.T.M., Gayed, S., Jahun, A., Hosmillo, M., Rees-Spear, C., Mlcochova, P., Lumb, I.U., et al.; CITIID-NIHR BioResource COVID-19 Collaboration; COVID-19 Genomics UK (COG-UK) Consortium (2021). SARS-CoV-2 evolution during treatment of chronic infection. Nature *592*, 277–282.

29. Zhang, L., Jackson, C.B., Mou, H., Ojha, A., Peng, H., Quinlan, B.D., Rangarajan, E.S., Pan, A., Vanderheiden, A., Suthar, M.S., et al. (2020). SARS-CoV-2 spike-protein D614G mutation increases virion spike density and infectivity. Nat. Commun. *11*, 6013.

30. Wu, K., Werner, A.P., Moliva, J.I., Koch, M., Choi, A., Stewart-Jones, G.B.E., Bennett, H., Boyoglu-Barnum, S., Shi, W., Graham, B.S., et al. (2021). mRNA-1273 vaccine induces neutralizing antibodies against spike mutants from global SARS-CoV-2 variants. bioRxiv. https://doi.org/10.1101/2021.01.25.427948.

31. Muik, A., Wallisch, A.K., Sänger, B., Swanson, K.A., Mühl, J., Chen, W., Cai, H., Maurus, D., Sarkar, R., Türeci, Ö., et al. (2021). Neutralization of SARS-CoV-2 lineage B.1.1.7 pseudovirus by BNT162b2 vaccine-elicited human sera. Science *371*, 1152–1153.

32. Wang, Z., Schmidt, F., Weisblum, Y., Muecksch, F., Barnes, C.O., Finkin, S., Schaefer-Babajew, D., Cipolla, M., Gaebler, C., Lieberman, J.A., et al. (2021). mRNA vaccine-elicited antibodies to SARS-CoV-2 and circulating variants. Nature *592*, 616–622.

33. Wang, P., Liu, L., Iketani, S., Luo, Y., Guo, Y., Wang, M., Yu, J., Zhang, B., Kwong, P.D., Graham, B.S., et al. (2021). Increased resistance of SARS-CoV-2 variants B.1.351 and B.1.1.7 to antibody neutralization. bioRxiv. https://doi.org/10.1101/2021.01.25.428137.

34. Mahase, E. (2021). COVID-19: Novavax vaccine efficacy is 86% against UK variant and 60% against South African variant. BMJ *372*, n296.

35. Shinde, V., Bhikha, S., Hoosain, Z., Archary, M., Bhorat, Q., Fairlie, L., Lalloo, U., Masilela, M.S.L., Moodley, D., Hanley, S., et al.; 2019nCoV-501 Study Group (2021). Efficacy of NVX-CoV2373 COVID-19 vaccine against the B.1.351 variant. N. Engl. J. Med. *384*, 1899–1909.

36. Korber, B., Fischer, W.M., Gnanakaran, S., Yoon, H., Theiler, J., Abfalterer, W., Hengartner, N., Giorgi, E.E., Bhattacharya, T., Foley, B., et al.; Sheffield COVID-19 Genomics Group (2020). Tracking changes in SARS-CoV-2 spike: evidence that D614G increases infectivity of the COVID-19 virus. Cell *182*, 812–827.e19.

37. Plotkin, S.A., and Halsey, N. (2021). Accelerate COVID-19 vaccine rollout by delaying the second dose of mRNA vaccines. Clin. Infect. Dis., ciab068.

38. Kadire, S.R., Wachter, R.M., and Lurie, N. (2021). Delayed second dose versus standard regimen for COVID-19 vaccination. N. Engl. J. Med. *384*, e28.

39. Matrajt, L., Eaton, J., Leung, T., Dimitrov, D., Schiffer, J.T., Swan, D.A., and Janes, H. (2021). Optimizing vaccine allocation for COVID-19 vaccines: critical role of single-dose vaccination. medRxiv. https://doi.org/10.1101/2020.12.31.20249099.

40. Emary, K.R.W., Golubchik, T., Aley, P.K., Ariani, C.V., Angus, B., Bibi, S., Blane, B., Bonsall, D., Cicconi, P., Charlton, S., et al.; COVID-19 Genomics UK consortium; AMPHEUS Project; Oxford COVID-19 Vaccine Trial Group (2021). Efficacy of ChAdOx1 nCoV-19 (AZD1222) vaccine against SARS-CoV-2 variant of concern 202012/01 (B.1.1.7): an exploratory analysis of a randomised controlled trial. Lancet *397*, 1351–1362.

41. Barrett, J.R., Belij-Rammerstorfer, S., Dold, C., Ewer, K.J., Folegatti, P.M., Gilbride, C., Halkerston, R., Hill, J., Jenkin, D., Stockdale, L., et al.; Oxford COVID Vaccine Trial Group (2021). Phase 1/2 trial of SARS-CoV-2 vaccine ChAdOx1 nCoV-19 with a booster dose induces multifunctional antibody responses. Nat. Med. *27*, 279–288.

42. Tauzin, A., Nayrac, M., Benlarbi, M., Gong, S.Y., Gasser, R., Beaudoin-Bussieres, G., Brassard, N., Laumaea, A., Vezina, D., Prevost, J., et al. (2021). A single BNT162b2 mRNA dose elicits antibodies with Fc-mediated effector functions and boost pre-existing humoral and T cell responses. bioRxiv. https://doi.org/10.1101/2021.03.18.435972.

43. Winkler, E.S., Gilchuk, P., Yu, J., Bailey, A.L., Chen, R.E., Chong, Z., Zost, S.J., Jang, H., Huang, Y., Allen, J.D., et al. (2021). Human neutralizing antibodies against SARS-CoV-2 require intact Fc effector functions for optimal therapeutic protection. Cell *184*, 1804–1820.e16.

44. Ullah, I., Prevost, J., Ladinsky, M.S., Stone, H., Lu, M., Anand, S.P., Beaudoin-Bussieres, G., Benlarbi, M., Ding, S., Gasser, R., et al. (2021). Live imaging of SARS-CoV-2 infection in mice reveals neutralizing antibodies require Fc function for optimal efficacy. bioRxiv. https://doi.org/10.1101/2021.03.22.436337.

45. Tortorici, M.A., Beltramello, M., Lempp, F.A., Pinto, D., Dang, H.V., Rosen, L.E., McCallum, M., Bowen, J., Minola, A., Jaconi, S., et al. (2020). Ultrapotent human antibodies protect against SARS-CoV-2 challenge via multiple mechanisms. Science *370*, 950–957.

46. Mahase, E. (2020). Covid-19: Pfizer vaccine efficacy was 52% after first dose and 95% after second dose, paper shows. BMJ *371*, m4826.

47. Bernal, J.L., Andrews, N., Gower, C., Stowe, J., Robertson, C., Tessier, E., Simmons, R., Cottrell, S., Roberts, R., O'Doherty, M., et al. (2021). Early effectiveness of COVID-19 vaccination with BNT162b2 mRNA vaccine and ChAdOx1 adenovirus vector vaccine on symptomatic disease, hospitalisations and mortality in older adults in England. medRxiv. https://doi.org/10.1101/2021.03.01.21252652.

48. Ledford, H. (2021). J&J's one-shot COVID vaccine offers hope for faster protection. Nature, Published online January 29, 2021. https://doi.org/10.1038/d41586-021-00119-7.

49. Iwasaki, A., Foxman, E.F., and Molony, R.D. (2017). Early local immune defences in the respiratory tract. Nat. Rev. Immunol. *17*, 7–20.

50. Subbarao, K., and Mahanty, S. (2020). Respiratory virus infections: understanding COVID-19. Immunity *52*, 905–909.

51. Sealy, R.E., Surman, S.L., Vogel, P., and Hurwitz, J.L. (2016). Antibody-secreting cells in respiratory tract tissues in the absence of eosinophils as supportive partners. Int. Immunol. *28*, 559–564.

52. Kato, A., Hulse, K.E., Tan, B.K., and Schleimer, R.P. (2013). B-lymphocyte lineage cells and the respiratory system. J. Allergy Clin. Immunol. *131*, 933–957, quiz 958.

53. Chiu, C., and Openshaw, P.J. (2015). Antiviral B cell and T cell immunity in the lungs. Nat. Immunol. *16*, 18–26.

54. Callaway, E. (2020). The coronavirus is mutating—does it matter? Nature *585*, 174–177.

55. Lee, C.Y.-P., Amrun, S.N., Chee, R.S.-L., Goh, Y.S., Mak, T.-M., Octavia, S., Yeo, N.K.-W., Chang, Z.W., Tay, M.Z., Torres-Ruesta, A., et al. (2020). Neutralizing antibodies from early cases of SARS-CoV-2 infection offer cross-protection against the SARS-CoV-2 D614G variant. bioRxiv. https://doi.org/10.1101/2020.10.08.332544.

56. Plante, J.A., Liu, Y., Liu, J., Xia, H., Johnson, B.A., Lokugamage, K.G., Zhang, X., Muruato, A.E., Zou, J., Fontes-Garfias, C.R., et al. (2021). Spike mutation D614G alters SARS-CoV-2 fitness. Nature *592*, 116–121.

57. Weissman, D., Alameh, M.G., de Silva, T., Collini, P., Hornsby, H., Brown, R., LaBranche, C.C., Edwards, R.J., Sutherland, L., Santra, S., et al. (2021). D614G spike mutation increases SARS CoV-2 susceptibility to neutralization. Cell Host Microbe *29*, 23–31.e4.

58. Starr, T.N., Greaney, A.J., Hilton, S.K., Ellis, D., Crawford, K.H.D., Dingens, A.S., Navarro, M.J., Bowen, J.E., Tortorici, M.A., Walls, A.C., et al. (2020). Deep mutational scanning of SARS-CoV-2 receptor binding domain reveals constraints on folding and ACE2 binding. Cell *182*, 1295–1310.e20.

59. Santos, J.C., and Passos, G.A. (2021). The high infectivity of SARS-CoV-2 B.1.1.7 is associated with increased interaction force between Spike-ACE2 caused by the viral N501Y mutation. bioRxiv. https://doi.org/10.1101/2020.12.29.424708.

60. Wibmer, C.K., Ayres, F., Hermanus, T., Madzivhandila, M., Kgagudi, P., Oosthuysen, B., Lambson, B.E., de Oliveira, T., Vermeulen, M., van der Berg, K., et al. (2021). SARS-CoV-2 501Y.V2 escapes neutralization by South African COVID-19 donor plasma. Nat. Med. *27*, 622–625.

61. Garcia-Beltran, W.F., Lam, E.C., St Denis, K., Nitido, A.D., Garcia, Z.H., Hauser, B.M., Feldman, J., Pavlovic, M.N., Gregory, D.J., Poznansky, M.C., et al. (2021). Multiple SARS-CoV-2 variants escape neutralization by vaccine-induced humoral immunity. Cell *184*, 2372–2383.e9.

62. Tegally, H., Wilkinson, E., Giovanetti, M., Iranzadeh, A., Fonseca, V., Giandhari, J., Doolabh, D., Pillay, S., San, E.J., Msomi, N., et al. (2020). Emergence and rapid spread of a new severe acute respiratory syndrome-related coronavirus 2 (SARS-CoV-2) lineage with multiple spike mutations in South Africa. medRxiv. https://doi.org/10.1101/2020.12.21.20248640.

63. Mahase, E. (2020). Covid-19: What have we learnt about the new variant in the UK? BMJ *371*, m4944.

64. Voloch, C.M., da Silva Francisco, R., Jr., de Almeida, L.G.P., Cardoso, C.C., Brustolini, O.J., Gerber, A.L., Guimarães, A.P.C., Mariani, D., da Costa, R.M., Ferreira, O.C., Jr., et al.; Covid19-UFRJ Workgroup, LNCC Workgroup, Adriana Cony Cavalcanti (2021). Genomic characterization of a novel SARS-CoV-2 lineage from Rio de Janeiro, Brazil. J. Virol. *95*, e00119-21.

65. Greaney, A.J., Starr, T.N., Gilchuk, P., Zost, S.J., Binshtein, E., Loes, A.N., Hilton, S.K., Huddleston, J., Eguia, R., Crawford, K.H.D., et al. (2021). Complete mapping of mutations to the SARS-CoV-2 spike receptor-binding domain that escape antibody recognition. Cell Host Microbe *29*, 44–57.e9.

66. Weisblum, Y., Schmidt, F., Zhang, F., DaSilva, J., Poston, D., Lorenzi, J.C., Muecksch, F., Rutkowska, M., Hoffmann, H.H., Michailidis, E., et al. (2020). Escape from neutralizing antibodies by SARS-CoV-2 spike protein variants. eLife *9*, e61312.

67. Shen, X., Tang, H., Pajon, R., Smith, G., Glenn, G.M., Shi, W., Korber, B., and Montefiori, D.C. (2021). Neutralization of SARS-CoV-2 variants B.1.429 and B.1.351. N. Engl. J. Med. *384*, 2352–2354.

68. Planas, D., Bruel, T., Grzelak, L., Guivel-Benhassine, F., Staropoli, I., Porrot, F., Planchais, C., Buchrieser, J., Rajah, M.M., Bishop, E., et al. (2021). Sensitivity of infectious SARS-CoV-2 B.1.1.7 and B.1.351 variants to neutralizing antibodies. Nat. Med. *27*, 917–924.

69. Zhou, D., Dejnirattisai, W., Supasa, P., Liu, C., Mentzer, A.J., Ginn, H.M., Zhao, Y., Duyvesteyn, H.M.E., Tuekprakhon, A., Nutalai, R., et al. (2021). Evidence of escape of SARS-CoV-2 variant B.1.351 from natural and vaccine-induced sera. Cell *184*, 2348–2361.e6.

70. Corey, L., Mascola, J.R., Fauci, A.S., and Collins, F.S. (2020). A strategic approach to COVID-19 vaccine R&D. Science *368*, 948–950.

71. Hodgson, S.H., Mansatta, K., Mallett, G., Harris, V., Emary, K.R.W., and Pollard, A.J. (2020). What defines an efficacious COVID-19 vaccine? a review of the challenges assessing the clinical efficacy of vaccines against SARS-CoV-2. Lancet Infect. Dis. *21*, e26–e35.

72. Chandrashekar, A., Liu, J., Martinot, A.J., McMahan, K., Mercado, N.B., Peter, L., Tostanoski, L.H., Yu, J., Maliga, Z., Nekorchuk, M., et al. (2020). SARS-CoV-2 infection protects against rechallenge in rhesus macaques. Science *369*, 812–817.

73. McMahan, K., Yu, J., Mercado, N.B., Loos, C., Tostanoski, L.H., Chandrashekar, A., Liu, J., Peter, L., Atyeo, C., Zhu, A., et al. (2021). Correlates of protection against SARS-CoV-2 in rhesus macaques. Nature *590*, 630–634.

74. Yu, J., Tostanoski, L.H., Mercado, N.B., McMahan, K., Liu, J., Jacob-Dolan, C., Chandrashekar, A., Atyeo, C., Martinez, D.R., Anioke, T., et al. (2021). Protective efficacy of Ad26.COV2.S against SARS-CoV-2 B.1.351 in macaques. Nature *596*, 423–427.

75. Alter, G., Yu, J., Liu, J., Chandrashekar, A., Borducchi, E.N., Tostanoski, L.H., McMahan, K., Jacob-Dolan, C., Martinez, D.R., Chang, A., et al. (2021). Immunogenicity of Ad26.COV2.S vaccine against SARS-CoV-2 variants in humans. Nature *596*, 268–272.

76. Lövgren, K., and Morein, B. (1988). The requirement of lipids for the formation of immunostimulating complexes (iscoms). Biotechnol. Appl. Biochem. *10*, 161–172.

77. Wrapp, D., Wang, N., Corbett, K.S., Goldsmith, J.A., Hsieh, C.L., Abiona, O., Graham, B.S., and McLellan, J.S. (2020). Cryo-EM structure of the 2019-nCoV spike in the prefusion conformation. Science *367*, 1260–1263.

78. Tian, J.H., Patel, N., Haupt, R., Zhou, H., Weston, S., Hammond, H., Logue, J., Portnoff, A.D., Norton, J., Guebre-Xabier, M., et al. (2021). SARS-CoV-2 spike glycoprotein vaccine candidate NVX-CoV2373 immunogenicity in baboons and protection in mice. Nat. Commun. *12*, 372.

79. Naldini, L., Blömer, U., Gage, F.H., Trono, D., and Verma, I.M. (1996). Efficient transfer, integration, and sustained long-term expression of the transgene in adult rat brains injected with a lentiviral vector. Proc. Natl. Acad. Sci. USA *93*, 11382–11388.

80. Butler, A.L., Fallon, J.K., and Alter, G. (2019). A sample-sparing multiplexed ADCP assay. Front. Immunol. *10*, 1851.

81. Karsten, C.B., Mehta, N., Shin, S.A., Diefenbach, T.J., Slein, M.D., Karpinski, W., Irvine, E.B., Broge, T., Suscovich, T.J., and Alter, G. (2019). A versatile high-throughput assay to characterize antibody-mediated neutrophil phagocytosis. J. Immunol. Methods *471*, 46–56.

82. Fischinger, S., Fallon, J.K., Michell, A.R., Broge, T., Suscovich, T.J., Streeck, H., and Alter, G. (2019). A high-throughput, bead-based, antigen-specific assay to assess the ability of antibodies to induce complement activation. J. Immunol. Methods *473*, 112630.

83. Gunn, B.M., Yu, W.H., Karim, M.M., Brannan, J.M., Herbert, A.S., Wec, A.Z., Halfmann, P.J., Fusco, M.L., Schendel, S.L., Gangavarapu, K., et al. (2018). A role for Fc function in therapeutic monoclonal antibody-mediated protection against Ebola virus. Cell Host Microbe *24*, 221–233.e5.

84. Brown, E.P., Licht, A.F., Dugast, A.S., Choi, I., Bailey-Kellogg, C., Alter, G., and Ackerman, M.E. (2012). High-throughput, multiplexed IgG subclassing of antigen-specific antibodies from clinical samples. J. Immunol. Methods *386*, 117–123.

85. Brown, E.P., Dowell, K.G., Boesch, A.W., Normandin, E., Mahan, A.E., Chu, T., Barouch, D.H., Bailey-Kellogg, C., Alter, G., and Ackerman, M.E. (2017). Multiplexed Fc array for evaluation of antigen-specific antibody effector profiles. J. Immunol. Methods *443*, 33–44.

STAR★METHODS

KEY RESOURCES TABLE

REAGENT or RESOURCE	SOURCE	IDENTIFIER
Antibodies		
Peroxidase (HRP)-conjugated mouse anti-monkey IgG	Southern Biotech	Cat# 4700-04; RRID: AB_2796068
mouse anti-monkey IgA	Bio-Rad	Cat# MCA2553; RRID: AB_770111
HRP-conjugated goat anti-mouse IgG	Southern Biotech	Cat# 1030-05; RRID: AB_2619742
HRP-conjugated mouse anti-histidine-tag IgG	Southern Biotech	Cat# 4603-05; RRID: AB_2819136
Anti-human CD107a	BD Biosciences	Cat# 555802; RRID: AB_396136
Anti-human CD16	BD Biosciences	Cat# 557758; RRID: AB_396864
Anti-human CD56	BD Biosciences	Cat# 557747; RRID: AB_396853
Anti-human CD3	BD Biosciences	Cat# 558117; RRID: AB_397038
Anti-human IFNγ	BD Biosciences	Cat# 340449; RRID: AB_400425
Anti-human MIP1β	BD Biosciences	Cat# 550078; RRID: AB_393549
Fluorescien-conjugated IgG fraction to guinea pig complement C3	MP Bio	Cat# 0855385; RRID: AB_2334913
Anti-human CD66- Pac Blue	BioLegend	Cat# 305112; RRID: AB_2563294
Bacterial and virus strains		
SARS-CoV-2 USA-WA1/2020	BEI Resources	NR-52281
Chemicals, peptides, and recombinant proteins		
EDC	Thermo Fisher Scientific	A35391
Sulfo-NHS	Thermo Fisher Scientific	A39269
EZ-link™ Sulfo-NHS-LC-LC-Biotin	Thermo Fisher Scientific	A35358
FluoSphere™ NeutrAvidin™ conjugated beads	Thermo Fisher Scientific	F8776 and F8775
Lyophilized Guinea Pig complement	Cedarlane	CL4051
Gelatin Veronal Buffer with calcium and magnesium	Boston bioproducts	IBB-300
Bovine Serum Albumin	Sigma	A2153
Spike	Dr. Erica Saphire	
SARS-CoV-2rS protein	Novavax, Inc.	BV2373
Histidine-tagged hACE2	Sino Biologics	10108-H08H
Receptor binding domain protein	Dr. Florian Krammer	
TBS Startingblock Blocking buffer	Thermo Fisher Scientific	37542
TMB	Sigma	T0440
TMB stop solution	ScyTek Laboratories	TSB125
Matrix-M™	Novavax	M1-111
TRIzol LS reagent	Thermo Fisher Scientific	10296010
Fugene 6	Promega	E2692
Golgistop	BD Bioscience	554724
Brefeldin A	sigma	B7651
4% PFA	SantaCruz Biotechnology	Sc-281692
Fix/Perm Cell Fixation and permeabilization kit	LifeTech	GAS001S100
TaqPathTM 1-Step RT-qPCR Master Mix	Thermo Fisher Scientific	A15299
QuikChange Lightning Site-Directed Mutagenesis kit	Agilent Technologies	210518
Experimental models: Cell lines		
Vero E6	ATCC	Cat# CRL-1586; RRID: CVCL_0574
THP-1	ATCC	Cat# TIB-202; RRID: CVCL_0006

(*Continued on next page*)

Continued

REAGENT or RESOURCE	SOURCE	IDENTIFIER
HEK293T/ACE2	Dr. Michael Farzan and Huihui Mu	N/A
HEK293T/17	ATCC	Cat# CRL-11268; RRID: CVCL_1926
Experimental models: Organisms/strains		
rhesus macaques (*Macaca mulatta*)	Envigo	#464
Oligonucleotides		
SUBGEN-FORWARD:	Integrated DNA Technologies (IDT)	5'-CGATCTCTTGTAGATCTGTTCTC-3'
E_Sarbeco_R2 Reverse Primer:	Integrated DNA Technologies (IDT)	5'-ATATTGCAGCAGTACGCACACA-3'
Probe (Thermo): FAM-MGB:	Thermo Fisher Scientific	5'-ACACTAGCCATCCTTACTGCGCTTCG-3'
Recombinant DNA		
Full-length Spike Wuhan-1 strain	Drs. Barney Graham and Kizzmekia Corbett	VRC7480
Software and algorithms		
Graph Pad Prism	Graph Pad	Prism 9
IntelliCyt ForeCyt	IntelliCyt Corporation	V8.1
R	R Foundation for Statistical Computing	4.0.2
Custom Code	Dr. Carolin Loos and Krista Pullen	https://github.com/LoosC/systemsseRology and https://github.com/krista-pullen/Cell-Reports-Medicine-NVX-CoV2373

RESOURCE AVAILABILITY

Lead contact

Further information and requests for resources and reagents should be directed to and will be fulfilled by the lead contact Dr. Galit Alter (galter@mgh.harvard.edu).

Materials availability

Spike proteins, RBD proteins, and other reagents generated in this study will be made available on request, but we may require a payment and/or a completed Materials Transfer Agreement if there is potential for commercial application.

Data and code availability

Data is available by requests and should be directed to the lead contact Dr. Galit Alter (galter@mgh.harvard.edu).

Custom code is available on Github https://github.com/LoosC/systemsseRology and https://github.com/krista-pullen/Cell-Reports-Medicine-NVX-CoV2373.

Any additional information required to reanalyze the data reported in this work paper is available from the Lead Contact upon request.

EXPERIMENTAL MODEL AND SUBJECT DETAILS

Animal studies

Twenty-four experimentally naive rhesus macaques (*Macaca mulatta*) of Chinese origin were sourced from Envigo (Alice, TX, USA). Animals were screened and determined to be negative for Simian Immunodeficiency Virus (SIV), Simian T-Lymphotropic Virus-1 (STLV-1), Simian Varicella Virus (SVV) and *Macacine herpesvirus* 1 (Herpes B virus), and Simian Retrovirus (SRV1 and SRV2) by polymerase chain reaction (PCR), and negative for *Trypanosoma cruzi.* Rectal swabs were collected and tested for Shigella, Campylobacter, Salmonella, and Yersinia. Pharyngeal swabs were used to test for *Bordetella bronchiseptica*. All animals were tested and verified to be negative for tuberculosis. Animals were randomly assigned to groups, with stratification across age and gender, using a computerized randomization procedure. Twenty-four (12 male and 12 female) rhesus macaques, within the age range of > 3 to $<$ 8-year-olds and weight range $\geq$ 3.60 kg to $\leq$ 10 kg, were randomized into four immunization groups and two placebo groups

Animals were housed individually in stainless steel cages with wire mesh bottoms. Animals were fed commercially available certified primate diet from Purina Mills 5048 (LabDiet) and provided water *ad libitum* from an institutional watering system that was analyzed monthly for impurities. Environmental conditions included 12 h light and 12 h dark cycle with controlled temperature (74°F ± 10°F) and humidity (30% to 70% RH). Cages were cleaned daily.

The vaccination phase of the study was performed in the Texas Biomed Animal Biosafety Level 2 (ABSL-2) facility. Following the immunization phase of the study, animals were transferred and acclimated for 7 days in the Texas Biomed ABSL-3 facility prior to challenge. Animals were monitored a minimum of twice daily for the duration of the study.

The immunization and challenge phases of the study complied with all applicable sections of the Final Rules of the Animal Welfare Act regulations (9 CFR Parts 1, 2, and 3) and *Guide for the Care and Use of Laboratory Animals - National Academy Press, Washington D. C. 8th Edition, 2011 (The Guide*). The study was conducted at the Texas Biomedical Research Institute (Texas Biomed, San Antonio, TX, USA), an AAALAC (Association for the Assessment and Accreditation of Laboratory Animal Care) accredited facility. The work was conducted in accordance with a protocol approved by Texas Biomed's Institutional Animal Care and Use Committee.

Human subjects

Samples were from the previously described Phase 1 vaccine study.[25] Healthy 18-59-year-old men and non-pregnant women were included in the study. Previously infected individuals were excluded. With the exception of 6 sentinel participants vaccinated in an open-label manner, the remaining 125 participants were randomly assigned to vaccine and placebo groups in a blinded fashion. All subjects signed informed consent and safety oversight was monitored by a data monitoring board. Details on the trial can be found at clinicaltrails.gov number NCT04368988.

Cell lines

Vero E6 cells were obtained from ATCC, CRL-1586 and maintained in Minimal Eagles Medium (MEM) supplemented with 10% fetal bovine serum (FBS), 1% glutamine, and 1% penicillin and streptomycin (P/S). THP-1 cells (ATCC TIB-202) maintained in Roswell Park Memorial Institute (RPMI) medium, supplemented with 10% FBS, 1% glutamine, 1% P/S, 1% HEPES, and 50μM β-ME. HEK293T/ACE2 cells were obtained from Drs. Michael Farzan and Huihui Mu at the Scripps Research Institute (Jupiter, FL, USA).

Viruses

For the challenge phase of the study, the SARS-CoV-2 (USA-WA-1/2020) passage 4 (P4) isolate was obtained from Biodefense and Emerging Infections Research Resource Repository (catalog number NR-52281, BEI Resources, GenBank accession number MN985325.1). For the *in vitro* neutralization assay, the SARS-CoV-2 (USA-WA-1/2020) isolate was obtained from the Center for Disease Control and provided by Dr. Matthew Frieman, University of Maryland.

METHOD DETAILS

Study blinding

This study was blinded (assignment to vaccinated/immunized versus placebo group) to avoid bias in evaluation, euthanasia, gross pathology assessment, and qRT-PCR assay outcome. All staff performing *in vitro* assays were blinded to the animal vaccine dosage and to whether the animal received vaccine or placebo while performing assays and analysis.

Study design

Twenty-four (12 male and 12 female) rhesus macaques, were randomized into four immunization groups and two placebo groups. Based on historical data, this number would be sufficient to observe virological and immunological differences. NVX-CoV2373 was formulated with 50 μg Matrix-M on the day of immunization. The placebo groups received formulation buffer. Groups 1 (1 male and 1 female) received placebo in two doses spaced 21 days apart (study day 0 and 21) and group 4 (1 male and 1 female) received placebo in one dose (study day 0). Group 2 (2 females and 3 males) received 5 μg NVX-CoV2373 + 50 μg Matrix-M and group 3 (2 females and 3 males) received 25 μg NVX-CoV2373 + 50 μg Matrix-M in two doses spaced 21 days apart (study day 0 and 21). Group 5 (3 females and 2 males) received 5 μg NVX-CoV2373 + 50 μg Matrix-M and group 6 (3 females and 2 males) received 25 μg NVX-CoV2373 + 50 μg Matrix-M in one dose (study day 0). Injections (0.5 mL) were administered in the thigh muscle. Matrix-M adjuvant was provided by Novavax, AB (lot number M1-111, Uppsala, SWE).[76]

Animals were sedated by intramuscular (IM) administration of Telazol (2-8 mg kg^{-1}, IM) prior to vaccination, collection of blood samples, virus challenge, collection of nasopharyngeal swabs, nasal washes, and bronchoalveolar lavage (BAL). For serologic assessments, serum was collected on study day 0 prior to immunization and day 21, and day 31 or 32 after the first immunization and stored at −80°C until assayed. Nasal washes, nasopharyngeal swabs, and BAL were collected on study day 31/32, prior to challenge.

NVX-CoV2373 spike glycoprotein

The SARS-CoV-2 S vaccine was constructed from the full-length, wild-type SARS-CoV-2 S glycoprotein based on the GenBank gene sequence MN908947 nucleotides 21563-25384. The native S protein was modified by mutating the putative furin cleavage site (682-RRAR-685 to 682-QQAQ-685) in the S1/S2 cleavage domain to confer protease resistance. Two additional proline amino acid substitutions were inserted at positions K986P and V987P (2P) within the heptad repeat 1 (HR1) domain to stabilize SARS-CoV-2 S in a prefusion conformation.[77] The synthetic transgene was codon optimized and engineered into the baculovirus vector (BV2373) for expression in *Spodoptera frugiperda* (Sf9) insect cells (GenScript, Piscataway, NJ, USA). NVX-CoV2373 spike trimers were detergent extracted from the plasma membrane with phosphate buffer containing TERGITOL NP-9, clarified by centrifugation, and purified by

TMAE anion exchange and lentil lectin affinity chromatography. Purified NVX-CoV2373 (547 μg mL^{-1}, lot number BV2373-16APR20) was formulated in 25 mM sodium phosphate (pH 7.2), 300 mM NaCl, and 0.02% (v/v) polysorbate and supplied frozen at −80°C ± 10°C.[78]

Anti-spike IgG and IgA ELISA

Serum, nasal wash, and BAL anti-SARS-CoV-2 spike (S) protein IgG titers were determined by ELISA. Briefly, 96-well plates (Thermo Fisher Scientific, Rochester, NY, USA) were coated with 1.0 μg mL^{-1} of SARS-CoV-2 S protein (BV2373, Lot# 16Apr20, Novavax, Inc. Gaithersburg, MD, USA). Plates were washed with phosphate buffered Tween (PBS-T) and non-specific binding was blocked with TBS Startingblock blocking buffer (Thermo Fisher Scientific, Rochester, NY, USA). Serum samples were serially diluted 3-fold starting with a 1:100 dilution and BAL and nasal wash samples were serially diluted 2-fold starting with a 1:2 dilution, then added to the coated plates and incubated at room temperature for 2 h. For IgG ELISA, plates were washed with PBS-T, then incubated with horseradish peroxidase (HRP)-conjugated mouse anti-monkey IgG (catalog number 4700-05, Southern Biotech, Birmingham, AL, USA) for 1 h. For IgA ELISA, plates were washed with PBS-T and mouse anti-monkey IgA (catalog number MCA2553, Bio-Rad, Hercules, CA, USA) was added for 1 h followed by washing with PBS-T, then incubation with HRP-conjugated goat anti-mouse IgG (catalog number 1030-05, Southern Biotech). Plates were then developed with 3,3′,5,5′-tetramethylbenzidine (TMB) peroxidase substrate (Sigma, St. Louis, MO, USA). Reactions were stopped with TMB stop solution (ScyTek Laboratories, Inc. Logan, UT, USA). Plates were read at OD 450 nm with a SpectraMax Plus plate reader (Molecular Devices, Sunnyvale, CA, USA). EC_{50} values and endpoint titer values were calculated by 4-parameter fitting using SoftMax Pro 6.5.1 GxP software. Individual animal anti-S IgG or IgA titers, and group geometric mean titer (GMT) and 95% confidence interval (95% CI) were plotted using GraphPad Prism 9.0 software. For serum titers below the assay lower limit of detection (LOD), a titer of < 100 (starting dilution) was reported and a value of "50" assigned to the sample to calculate the group mean titer. For BAL and nasal wash titers below the assay LOD, a titer of < 2 (starting dilution) was reported and a value of "1" assigned to the sample to calculate the group mean titer.

Human angiotensin converting enzyme 2 (hACE2) receptor blocking antibody

Human ACE2 receptor blocking antibody titer was determined by ELISA. Ninety-six well plates were coated with 1.0 μg mL^{-1} SARS-CoV-2 rS protein (BV2373, lot no. 16Apr20, Novavax, Inc., Gaithersburg, MD, USA) overnight at 4°C. Sera were serially diluted 2-fold starting with a 1:20 dilution and were added to coated wells for 1 h at room temperature. After washing, 30 ng mL^{-1} histidine-tagged human ACE2 (Sino Biologics, Beijing, CHN) was added to wells for 1 h at room temperature. HRP-conjugated mouse anti-histidine-tag IgG (1:4000) (catalog number 4603-05, Southern Biotech, Birmingham, AL, USA) was added for 1 h followed by addition of TMB substrate. Plates were read at OD 450 nm with a SpectraMax Plus plate reader (Molecular Devices, Sunnyvale, CA, USA) and data analyzed with SoftMax Pro 6.5.1 GxP software. The % Inhibition for each dilution for each sample was calculated using the following equation in the SoftMax Pro program: 100-[(MeanResults/ControlValue@PositiveControl)*100].

Serum dilution versus % Inhibition plot was generated, and curve fitting was performed by 4-parameter logistic (4PL) curve fitting to data. Serum antibody titer at 50% inhibition (IC_{50}) of hACE2 to SARS-CoV-2 S protein was determined in the SoftMax Pro program. The group GMT and 95% CI and individual animal titers were plotted using GraphPad Prism 9.0 software. For a titer below the assay lower limit of detection (LOD), a titer of < 20 (starting dilution) was reported and a value of "10" assigned to the sample to calculate the group mean titer.

SARS-CoV-2 neutralizing antibody assay

The SARS-CoV-2 neutralizing antibody assay was conducted in a select agent ABSL-3 containment facility at the University of Maryland, School of Medicine. Sera were diluted 1:20 in Vero E6 cell growth media and further serially diluted 1:2 to 1:40,960. SARS-CoV-2 (multiplicity of infection (MOI) of 0.01 pfu per cell) was added to the wells for 60 min at 37°C. Vero E6 media was used as a negative control. Each serum dilution was assessed microscopically for inhibition of virus cytopathic effect (CPE) on Vero E6 cells. The endpoint titer was reported as the reciprocal of the dilution at which 99% CPE was observed at 3 days post infection.[25,78]

Preparation of the SARS-CoV-2 challenge stock

A fourth cell-culture passage (P4) of SARS-CoV-2 isolate USA-WA1/2020 was obtained from Biodefense and Emerging Infections Research Resources Repository (catalog number NR-52281, BEI Resources, GenBank accession number MN985325.1). Live virus stock was prepared in the Texas Biomed ABSL-3 containment facility. The stock virus was passaged for a fifth time (P5) in Vero E6 cells at a MOI of 0.001 to produce the master virus stock. The master stock was again passaged in Vero E6 cells at a MOI of 0.02 (P6) to produce the challenge stock. The P6 challenge stock had a titer of 2.10×10^6 pfu mL^{-1} (Lot No. 20200320) and was stored 500 μL aliquots at −65°C in Dulbecco's modified essential media (DMEM) and 10% fetal bovine serum. The identity of the challenge stock was confirmed to be SARS-CoV-2 by deep sequencing and was confirmed to be identical to the published sequence (GenBank: MN985325).

SARS-CoV-2 challenge

Vaccinated and placebo animals were transferred from the ABSL-2 facility on study day 31/32 to the ABSL-3 facility and acclimated for 7 days. On the day of challenge (study day 38), animals were sedated and challenged with a total target dose of 1.05×10^6 pfu in

500 μL. The challenge dose was equally administered by the intranasal (IN) route 5.25×10^5 pfu in 250 μL and intra-tracheal (IT) route 5.25×10^5 pfu in 250 μL. IN administration was performed with an atomization device (Teleflex Intranasal Mucosal Atomization Device LMA MAD Nasal Device, Morrisville, NC, USA) and IT delivery was performed with Tracheal Mucosal Atomization Device (Teleflex Laryngo-Tracheal Mucosal Atomization Device LMA MADGIC, Morrisville, NC, USA). To confirm the challenge dose, aliquots of the challenge samples were collected prior to challenging the first animal and last animal and stored at $\leq -65°C$. A neutral red agarose overlay and conventional plaque assay were used to confirm the titer of the challenge dose. The actual pre- and post-challenge titers were 1.80×10^6 pfu mL^{-1} and 7.83×10^5 pfu, respectively.

Sample collection for SARS-CoV-2 RNA quantification

Nasopharyngeal swab collection

Animals were sedated and nasopharyngeal swabs were collected prior to challenge (study day 31/32) and on 2, 3, 4, 6, and 7-8 days post infection (dpi). After collection, swabs were placed in a tube containing viral transport medium (VTM), then stored at $\leq -60°C$ until processing.

Bronchoalveolar lavage (BAL) collection

BAL aspirates were collected prior to challenge (study day 31/32) and on 2, 4 and 7-8 dpi. Animals were sedated and the trachea visualized with a laryngoscope. A sterile rubber feeding tube with stylet was inserted into the trachea and into the airway until it met slight resistance. Up to 80 mL of warm (< 40°C) sterile saline, divided into multiple aliquots, was instilled through the tube. Aspirated fluid was dispensed into sterile vials with VTM and stored at $\leq -60°C$ until batch processed.

Nasal wash collection

Nasal washes were collected prior to infection (study day 31/32) and 2, 4, and 7-8 dpi. Animals were sedated and a syringe with a flexible tipped 20-22-gauge intravenous (IV) catheter was inserted into the nostril passage and a volume of 2.5-5mL of sterile saline instilled. Samples were collected in sterile conical tubes containing VTM and stored at $\leq -60°C$ until batch processed.

Tissue collection

Tissues were collected 7-8 dpi (study days 45-46) at the scheduled necropsy from the upper, middle and lower lobes of the lung; nasal cavity; and trachea. Tissues were weighed and stored at $80°C \pm 10°C$ until batch processed. RNA was extracted analyzed for the presence of SARS-CoV-2 RNA via qRT-PCR targeting the N1 gene.

Quantification of virus load in nasopharyngeal swabs, nasal washes, BAL, and tissues

Genomic (g)RNA virus

Samples were assessed for viral load by qRT-PCR. A 250 μL aliquot of VTM inactivated in TRIzol LS reagent (catalog number 10296010, ThermoFisher Scientific) was used for isolation of total RNA. For total viral RNA, qRT-PCR targeting the nucleocapsid gene (N1) was run on duplicate samples and results reported as genome equivalents (GE) mL^{-1} for nasal washes/swabs and BAL. For tissue samples, results are reported as GE μg^{-1} for tissue homogenates.

Subgenomic (sg)RNA virus

Replicating virus load by qRT-PCR targeting the subgenomic envelope (E) gene RNA in 250 μL aliquot of nasopharyngeal swabs, nasal washes, and BAL aspirates. The forward and reverse primers, probe, cycling conditions, and Master Mix included:

SUBGEN-FORWARD: 5'-CGATCTCTTGTAGATCTGTTCTC-3'
E_Sarbeco_R2 Reverse Primer: 5'-ATATTGCAGCAGTACGCACACA-3'
Probe (Thermo): FAM-MGB: 5'-ACACTAGCCATCCTTACTGCGCTTCG-3'
TaqPath 1-Step RT-qPCR Master Mix, CG (catalog number A15299, ThermoFisher Scientific). Cycling parameters were 25°C 2 min, 50°C 15 min, 95°C 2 min; Amplification 40 × 95°C 3 s, 60°C 30 s.

Pseudovirus neutralizing antibody assay

SARS-CoV-2 neutralization was assessed with spike-pseudotyped virus infection of HEK293T/ACE2 cells as a function of reduction in luciferase (Luc) reporter activity. HEK293T/ACE2 cells were maintained in DMEM containing 10% fetal bovine serum, 25 mM HEPES, 50 μg mL^{-1} gentamycin and 3 μg mL^{-1} puromycin. An expression plasmid encoding codon-optimized full-length spike of the Wuhan-1 strain (VRC7480), was provided by Drs. Barney Graham and Kizzmekia Corbett at the Vaccine Research Center, National Institutes of Health (USA). The D614G amino acid change was introduced into VRC7480 by site-directed mutagenesis using the QuikChange Lightning Site-Directed Mutagenesis Kit (catalog number 210518, Agilent Technologies). The mutation was confirmed by full-length spike gene sequencing. Pseudovirions were produced in HEK293T/17 cells (ATCC cat. no. CRL-11268, Manassas, VA, USA) by transfection using Fugene 6 (catalog number E2692, Promega, Madison, WI, USA) and a combination of spike plasmid, lentiviral backbone plasmid (pCMV ΔR8.2) and firefly Luc reporter gene plasmid (pHR' CMV Luc) in a 1:17:17 ratio.[79] Transfections were allowed to proceed for 16-20 h at 37°C. Medium was removed, monolayers rinsed with growth medium, and 15 mL of fresh growth medium added. Pseudovirus-containing culture medium was collected after an additional 2 days of incubation and was clarified of cells by low-speed centrifugation and 0.45μm micron filtration and stored in aliquots at −80°C. $TCID_{50}$ assays were performed on thawed aliquots to determine the infectious dose for neutralization assays (RLU 500-1000x background, background 50-100 RLU).

For neutralization, a pre-titrated dose of virus was incubated with 8 serial 5-fold dilutions of serum samples in duplicate in a total volume of 150 μL for 1 h at 37°C in 96-well flat-bottom poly-L-lysine-coated Biocoat plates (catalog number 354461, Corning, NY,

USA). Cells were suspended using TrypLE Select Enzyme solution (Thermo Fisher Scientific) and immediately added to all wells (10,000 cells in 100 μL of growth medium per well). One set of 8 control wells received cells + virus (virus control) and another set of 8 wells received cells only (background control). After 66-72 h of incubation, medium was removed by gentle aspiration and 30 μL of Promega 1X lysis buffer was added to all wells. After a 10 min incubation at room temperature, 100 μL of Bright-Glo luciferase reagent was added to all wells. After 1-2 min, 110 μL of the cell lysate was transferred to a black/white plate (Perkin-Elmer). Luminescence was measured using a PerkinElmer Life Sciences, Model Victor2 luminometer. Neutralization titers are the serum dilution at which relative luminescence units (RLU) were reduced by either 50% (ID_{50}) compared to virus control wells after subtraction of background RLUs. Serum samples were heat-inactivated for 30 min at 56°C prior to assay.

Antibody-dependent cellular phagocytosis and neutrophil phagocytosis

ADCP and ADNP were conducted as previously described.[80,81] Briefly, NVX-CoV2373 Spike protein was biotinylated using EZ-link-™Sulfo-NHS-LC-LC-Biotin (Thermo Fisher), and then coupled to yellow/green FluoSphere™ NeutrAvidin™-conjugated beads (Thermo Fisher, F8776). Immune complexes were formed by incubating the bead+protein conjugates with diluted serum (ADNP 1:50 dilution, ADCP 1:100 dilution) for 2 h at 37°C, and then washed to remove unbound antibody. The immune complexes were then incubated overnight with THP-1 cells (ADCP), or for 1 h with RBC-lysed whole blood (ADNP). THP-1 cells were then washed and fixed in 4% PFA, while the RBC-lysed whole blood was washed, stained for CD66b+ (Biolegend) to identify neutrophils, and then fixed in 4% PFA. Flow cytometry was performed to identify the percentage of quantity of beads phagocytosed by THP-1 cells or neutrophils, and a phagocytosis score was calculated (% cells positive × Median Fluorescent Intensity of positive cells). Flow cytometry was performed with an iQue (IntelliCyt) or LSRII(BD) and analysis was performed using IntelliCyt ForeCyt (v8.1) or FlowJo V10.7.1 (Figure S1).

Antibody-dependent complement deposition

ADCD was conducted as previously described.[82] Briefly, NVX-CoV2373 Spike protein was biotinylated using EZ-link™Sulfo-NHS-LC-LC-Biotin (Thermo Fisher), and then coupled to red FluoSphere™ NeutrAvidin™-conjugated beads (Thermo Fisher). Immune complexes were formed by incubating the bead+protein conjugates with diluted serum (ADCD 1:10 dilution) for 2 h at 37°C, and then washed to remove unbound antibody. The immune complexes were then incubated with lyophilized guinea pig complement (Cedarlane) and diluted in gelatin veronal buffer with calcium and magnesium (Boston Bioproducts) for 30 min. C3 bound to immune complexes was detected by fluorescein-conjugated goat IgG fraction to guinea pig Complement C3 (MP Biomedicals). Flow cytometry was performed to identify the percentage of beads with bound C3. Flow cytometry was performed with an IQue (Intellicyt) and analysis was performed on IntelliCyt ForeCyt (v8.1) (Figure S1).

Antibody-dependent NK cell degranulation

Antibody-dependent NK cell degranulation was conducted as previously described.[83] NVX-CoV2373 Spike protein was coated on Maxisorp ELISA plate (Thermo Fisher), and then blocked with 5% BSA. Diluted serum (1:25 dilution) was then added and incubated for 2 h at 37°C. Human NK cells were isolated from peripheral blood by negative selection using the RosetteSep Human NK cell enrichment cocktail following the manufacturer's instructions. Human NK cells were then added to the bound antibody and incubated for 5 h at 37°C in the presence of RPMI+10%FBS, GolgiStop (BD), Brefeldin A (Sigma), and anti-human CD107a antibody (BD Bioscience). After incubation, cells were washed, stained with CD16, CD56, and CD3 (BD Bioscience), and fixed in 4% PFA for 15 min. Intracellular staining was performed using the FIX/PERM Cell fixation and permeabilization kit (Thermo), and cells were stained for interferon-γ and macrophage inflammatory protein-1β (BD bioscience). Flow cytometry was performed with an iQue (IntelliCyt) and analysis was performed on IntelliCyt ForeCyt (v8.1) (Figure S1).

Isotype and FcR-binding Luminex profiling

Isotyping and FcR profiling was conducted as previously described.[84,85] Briefly, antigens (NVX-CoV2373 Spike, SARS-CoV-2 Spike, S1, RBD, S2, HKU-1 RBD, or OC43 RBD) were carboxyl coupled to magnetic Luminex microplex carboxylated beads (Luminex Corporation) using NHS-ester linkages with Sulfo-NHS and EDC (Thermo Fisher), and then incubated with serum (Isotypes 1:100 dilution, FcRs 1:1000 dilution) for 2 h at 37°C. Isotyping was performed by incubating the immune complexes with secondary mouse-anti-rhesus antibody detectors for each isotype (IgG1, IgG2, IgG3, IgG4, IgA), then detected with tertiary anti-mouse-IgG antibodies conjugated to PE. FcR binding was quantified by incubating immune complexes with biotinylated FcRs (FcγR2A-1, FcγR2A-2, FcγR3A, courtesy of Duke Protein Production Facility) conjugated to Steptavidin-PE (Prozyme). Flow cytometry was performed with an iQue (IntelliCyt) and analysis was performed on IntelliCyt ForeCyt (v8.1) (Figure S1).

QUANTIFICATION AND STATISTICAL ANALYSIS

Statistical analyses were performed with GraphPad Prism 9.0 software. Serum antibodies were plotted for individual animals and the geometric mean titer (GMT) and 95% confidence intervals plotted. Virus loads were plotted as the median value, interquartile range, and minimum and maximum values. Student's t test or two-way ANOVA was used to determine differences between paired groups as indicated in the figure legends. $p \leq 0.05$ was considered significant. The AUCs and bootstrap confidence intervals

were calculated using the R package 'pROC'. For the case of AUC = 1 no confidence interval was provided. To calculate p values, the R package 'stats' was used. The AUC and fold change analyses were performed in R version 4.0.2.

Principal component analysis (PCA) and partial least square discriminant analysis were performed based on serological features using the R package 'ropls'. The systems serology antibody titers, FcR binding and ADCD measurements were log10-transformed, and all measurements were z-scored. The multivariate analyses were performed in R version 4.0.2.

Multiplate comparison and aggregated group analysis were used when appropriate to avoid statistical errors. Specific numbers of animals can be found in correspond figure legends. p values correlate with symbals as follows: Not significant (ns), *$p \leq 0.05$, **$p \leq 0.01$, ***$p \leq 0.001$, ****$p \leq 0.0001$.

ADDITIONAL RESOURCES

Details on the human subjects from the prior published trial[25] can be found at clinicaltrails.gov identifier: NCT04368988 https://clinicaltrials.gov/ct2/show/NCT04368988.

Cell Reports Medicine, Volume *2*

Supplemental information

Fab and Fc contribute to maximal protection against SARS-CoV-2 following NVX-CoV2373 subunit vaccine with Matrix-M vaccination

Matthew J. Gorman, Nita Patel, Mimi Guebre-Xabier, Alex L. Zhu, Caroline Atyeo, Krista M. Pullen, Carolin Loos, Yenny Goez-Gazi, Ricardo Carrion Jr., Jing-Hui Tian, Dansu Yuan, Kathryn A. Bowman, Bin Zhou, Sonia Maciejewski, Marisa E. McGrath, James Logue, Matthew B. Frieman, David Montefiori, Colin Mann, Sharon Schendel, Fatima Amanat, Florian Krammer, Erica Ollmann Saphire, Douglas A. Lauffenburger, Ann M. Greene, Alyse D. Portnoff, Michael J. Massare, Larry Ellingsworth, Gregory Glenn, Gale Smith, and Galit Alter

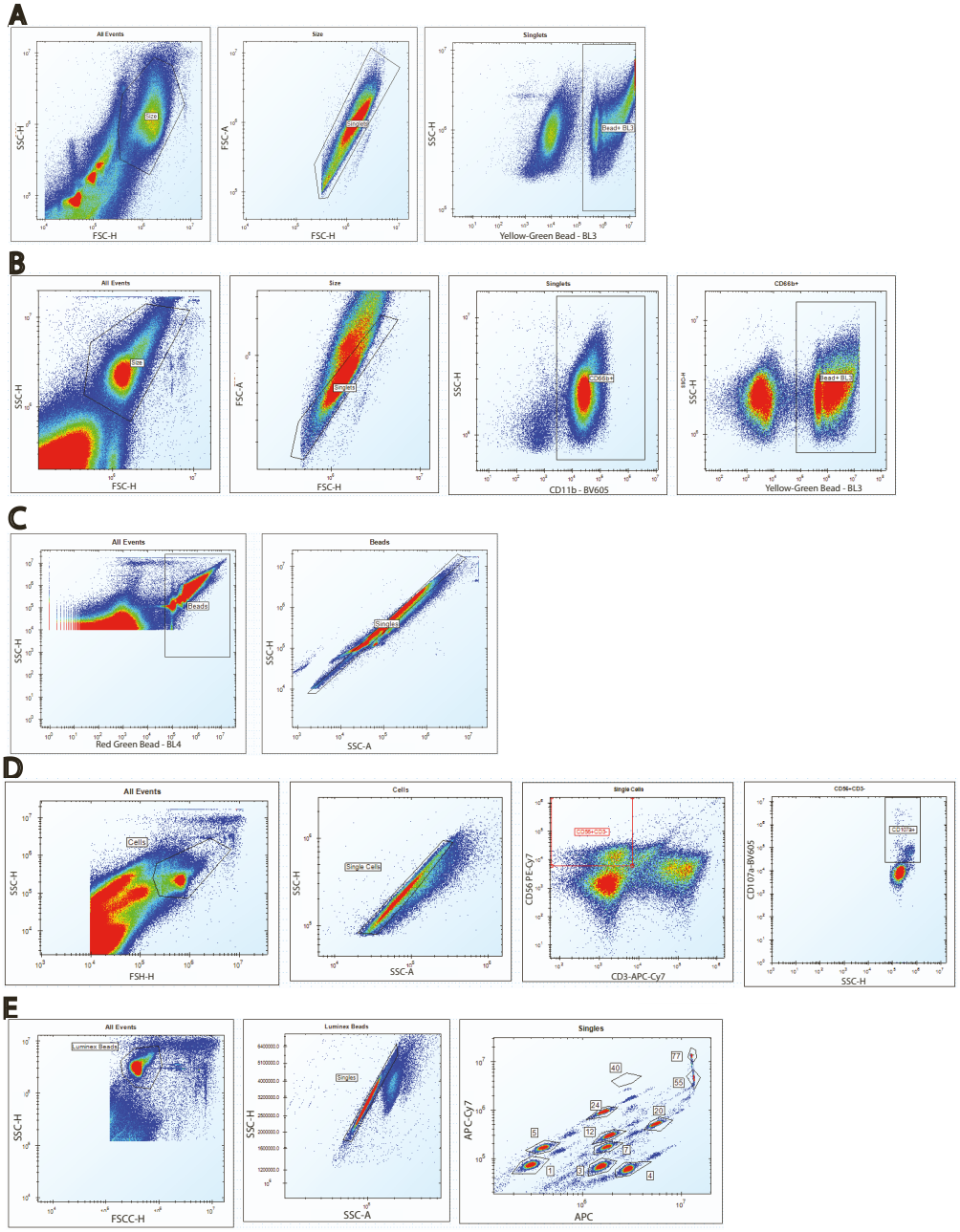

Supplementary Figure 1. Gating strategy for flow cytometry, Related to Figure 3.
Example of flow cytometry gating scheme for (A) antibody-dependent cellular phagocytosis (ADCP), (B) antibody-dependent neutrophil phagocytosis (ADNP), (C) antibody-dependent complement deposition (ADCD), (D) antibody-dependent NK degranulation (measured by CD107%) (NKdegran), and (E) Luminex.